European Development and Research Academy

Journal of Natural and Applied Sciences *Ural*

Center for Research and Development of Human Resources Ramah- Jordan

ISSN (Print): 2958-8987

ISSN (Online): 2958-8995

No: 1 Val:1/ November / 2022

Journal of Natural and Applied Sciences URAL

A Quarterly Multidisciplinary Scientific Journal Issued by Center of Research and Human Resources Development Ramah- Jordan and European Development and Research Academy/ Brussels

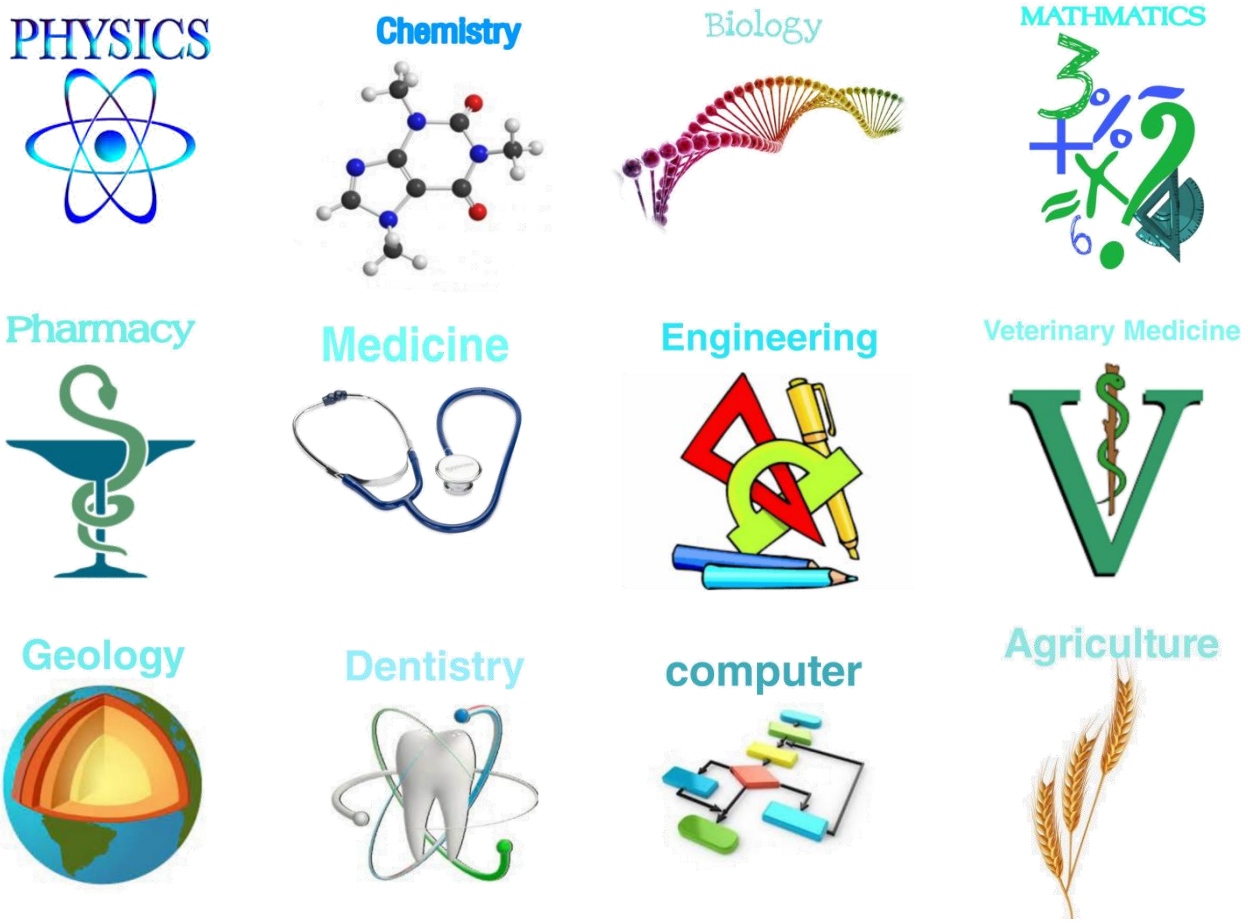

The Publication Terms

- The researcher submits a pledge not to send the research to any other journal, as well as not to participate the research in any scientific conference.
- The total number of research pages must not exceed 15 pages, and the abstract of the research must be written in the research language only.
- The title of the research should be written in bold, size 16. The name of the researcher or researchers should be written in bold 12. The affiliation of the researcher should be in a plain, non-bold font 12. The researcher's email should be attached under it.
- Headlines within the research should be written in bold in 12, and the content should written in 12. The table-title should be centered line at the top line of the table.
- The title of the figures and images is in the middle of the line below the figure or the image. The word sources should be in bold 12 and all the sources are written in 10 font, and the font is Times New Roman for all researches, whether in Arabic or English. The spacing is single and not more than 1.
- The Vancouver system must be followed in citing and writing sources where the source number should be written inside the body between square brackets [ ] and the sources are serialized in the list of sources according to the order of the source in the body of the research.
- Research submissions are printed in a Microsoft Word file.
- The journal has all intellectual property rights to the published research.
- The published research does not express only the opinions of its owners.
- The editorial board has the right to make some formal modifications to the submitted article when necessary without changing the content of the topic.

Introduction to the First Issue

In the name of Allah, the most Compassionate, the most Merciful

It is my pleasure to offer researchers the opportunity to publish their valuable scientific research that serves the natural and applied sciences and develops them for the better.

The journal staff promise the researchers to develop the work in order to get in the global capacities and it will be one of the best regional and global journals

We present this first issue between your hands
As we appreciate the efforts of the journal staff

Prof . Dr. Ghassan Ezzedin Aref

Editor-in-Chief

Publication specializations in the journal	
Biology	Chemistry
Physics	Geology
Computer	Agriculture
Engineering	Mathematics
Medicine	Pharmacy
Veterinary	Dentistry
Environment	Nursing

The journal is published in English and Arabic

General Supervisor of the Journal:

Prof. Khalid Ragheb Ahmed Al-Khatib

Head of the Center for Research and Human

Resources Development Ramah – Jordan

Managing Director:

Dr. Mosaddaq Ameen Ateah AL- Doori

Administrative title of the journal:

Amman\ Jordan\ Wasfi Al-Tal \ Gardens

Phone: +962799424774

Index

Seq.	Research Title	Researcher	Page
1.	Identification of water quality in Radoum Area-South Darfur-Sudan	Zeinab. A.A.E.Elrabei-department of chemistry-faculty of Education-University of Nyala-Sudan	5 - 18
2.	Depth Prevalence of Petroleum Residue in Different Soil Texture	Assist. Prof. Baraa Mohammed Ibrahim Al-Hilali\ Biology Department, College of Education, University of Samarra, Iraq	22 - 27
3.	Physics and Procedure of Gamma knife Radiosurgery	Assis. Techer. Alyaa Hussein Ashour *University of Mashreq, Baghdad, Iraq*	30 - 46
4.	An Application on Principal Components Analysis using R	Qasim N.Husain and Alaa M.Dedaa Department of Mathematics, College of Education for Pure Sciences, Tikrit University, Tikrit ,IRAQ	45-55

ISSN (Print): 2958-8987
ISSN (Online): 2958-8995
Doi: 10.59799/APPP6605

Identification of water quality in Radoum Area-South Darfur-Sudan

دراسة ومعرفة جودة المياه بمنطقة الردوم ولاية جنوب دارفور-السودان

Zeinab. A.A.E.Elrabei-department of chemistry-faculty of Education-University of Nyala-Sudan

ملخص

يهدف هذا البحث إلى دراسة ومعرفة جودة المياه بمنطقة الردوم ولاية جنوب دارفور. تم جمع عينات المياه من مصادر مختلفة خلال موسمي الصيف والخريف، وتم تحليل هذه العينات باستخدام جهاز الامتصاص الذرى وطرق المعايرة التقليدية. تم استخدام العديد من البرامج الحاسوبية لتحليل وتفسير البيانات مثل .aqua chem.,SPSS

من نتائج التحليل وجد ان تركيز كاتيون الصوديوم متبوعا بكتيون الكالسيوم ثم المغنيسيوم هى الكاتيونات السائدة فى العينات بينما الانيونات السائدة هي البيكربونات والكلوريدات والكبريتات على التوالى.

معدل الارتباط(المضاهاة) المتوسطة بين كاتيونات الصوديوم وانيونات البيكربونات ترجع الى تواجد معدن الثيرمونترايت ($Na_2CO_3H_2O$) ومعدن الهالايت في وضع تحتNacl التشبع .معدل الارتباط المتوسط الى القوى بين كاتيونات المغنيسيوم والكالسيوم مع انيونات البيكربونات تشير الى تواجد صخور الدولومايت وصخور الكربونيات بمنطقة الدراسة.المضاهاة الجزئية بين الكاتيونات و الانيونات الأساسية تظهر انحلال وخلط بسيطين ويعزى هذا الى عدم وجود ارتباط قوى واضح بين الكاتيونات والايونات الرئيسية.

وباستخدام التصنيف الاحصائى المتعدد للعينات فى موسمي الصيف والخريف تم تصنيف العينات الى ثلاث مجموعات متجانسة إحصائيا. وباستخدام المزيد من التحليل الاحصائى تم تقسيم هذه المجموعات العدد من المكونات المميزة في موسمي الصيف والخريف.

بمقارنة العينات إحصائيا فى موسم الخريف والصيف بمنطقة الدراسة لوحظ عدم وجود فارق ملحوظ بين متوسطات تركيز العناصر الرئيسية في موسمي الدراسة.

Abstract:

This study aims at assessing the identification of water quality in Radoum Area-South Darfur-Sudan. Water samples were collected from different sources in wet and dry seasons, and analyses using atomic absorption, and traditional titration techniques. Different computer software's were used to analyses and interpret ate data such as Aqua chem and SPSS. From the analyses data sodium followed by calcium and magnesium were the main dominant cations, while bicarbonate followed by chloride and sulphide were the dominant anions in wet and dry seasons. The moderately established correlation between sodium and bicarbonate is due to the presence of thermonatrite ($Na_2CO_3 H2O$) and halite (NaCl) in under saturated state. The moderate to strong correlation between magnesium, calcium and bicarbonate indicate of presences of dolomite and carbonate rocks in the study area. The partial correlation between major cations and major anions showed that the water exhibits simple dissolution or mixing processes due to no dominancy of an anion and/or a cation. Multi variant classifications of water samples in dry and wet seasons have resulted into three homogenous clusters (group). Further Classification by Factor analysis indicates three components responsible of the variation with the data area in wet and dry seasons. between the mean concentrations of the different parameter in wet and dry seasons in the study area shows that there are no significant differences between the mean concentrations of all the studied variables.

Keywords: - Radoum area, SPSS. Correlation, atomic absorption, water quality

1-Introduction

Water is the major chemical component and universal solvent of living systems. It makes to up about 70 percent of human body weight and is the principal medium for metabolic processes (Nason, 1965). Water that exists today has been on earth for billions of years. Water covers four-fifth of our world**. (**Armand, 1965). More than 80% of the earth's surface is covered by water, but less than 1 % of it is fresh and/ or drinkable water**.**

1.2 Composition of water:

Pure water consists of two parts of hydrogen and one part of oxygen by volume, and one part of hydrogen and eight parts of oxygen by weight. **(**Armand, 1965).

1.3 Impurities:

No water on earth is 100% pure. It acquires several types of impurities in passage from its origin to place of consumption. (Bsnraju, 1995).

2-Significance of the problem: -

The area is known of its mineralization, including trace minerals. And as water is hosted and moves in these rocks, interacts with the minerals constituted in the rocks, and consequently effect ground water. In most cases the chemical constituents of a ground water sample are an indicator of the chemical composition and the type of the source rocks. On the other hand, seasonal streams (Khors) are sources of surface and/ or perched ground water supply. Traditional shallow wells (Masheesh) are dug on the beds of the khors to tap perched ground water. The khors in the area originate from the high lands of the basement terrains and mostly aligned with the fracture lines trending NE. The area is characterized by its high rainfalls, which produce channel and sheet runoffs. As water flow through these channels encroaches rocks/soil, dissolves, removes and deposits materials that effect physical and chemical properties of surface and ground water. Persumenbly, seasonal climate variations (wet &dry) cause some variations in the properties of water samples measured in different seasons, reflecting the effect of the mineralization in the area.

3-Objectives:

The overall objective of the study is to detect the water quality in study area.

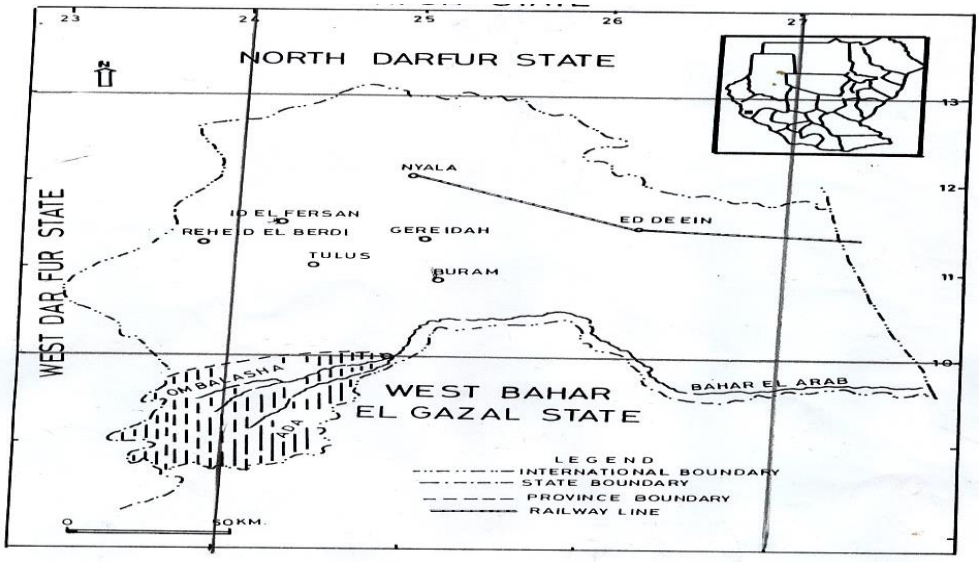

Fig (1) Location map of study area

4-Physiograhical Features.

4.1-Topography:

The regional topography of the area comprises high lands on its south western limits the area which stands at an average elevation of about 1240m above sea level. The higher lands merge into a vast plain as low as

438 m towards Hofrat Enhas area NE wards. However, a number of isolated hillocks and low-lying ridges are not uncommon.

4.2-Drainage:

Generally, the area lies within Nile drainage basin. There are many seasonal streams that drain the area in NE and SE. Bahr ElArab is considered as the main river in the area, it has two branches: Adda River, and Um Blacha River (Fig2). The two branches of Bahr ElArab come from Central Africa and temporary flow according to the rainy season, and usually effected by the sand deposit**s** (Abo Elzaki, 2006). Most of the drainage pattren which feeds the Um blacha river is located to the south of draining to the north-eastern direction. The tributaries include Neher Adda, Neher Umblacha, Wadi Foungo,Wadi Raikakai and Wadi Shlakha and all of them are characterized by a complicated system of meanderings and ox-bows indicating maturity. Some parts of these streams turn into swamps rather than defined channels especially during the rainy seasons. This is the flatness (low gradients) at lower reaches and sluggish flow

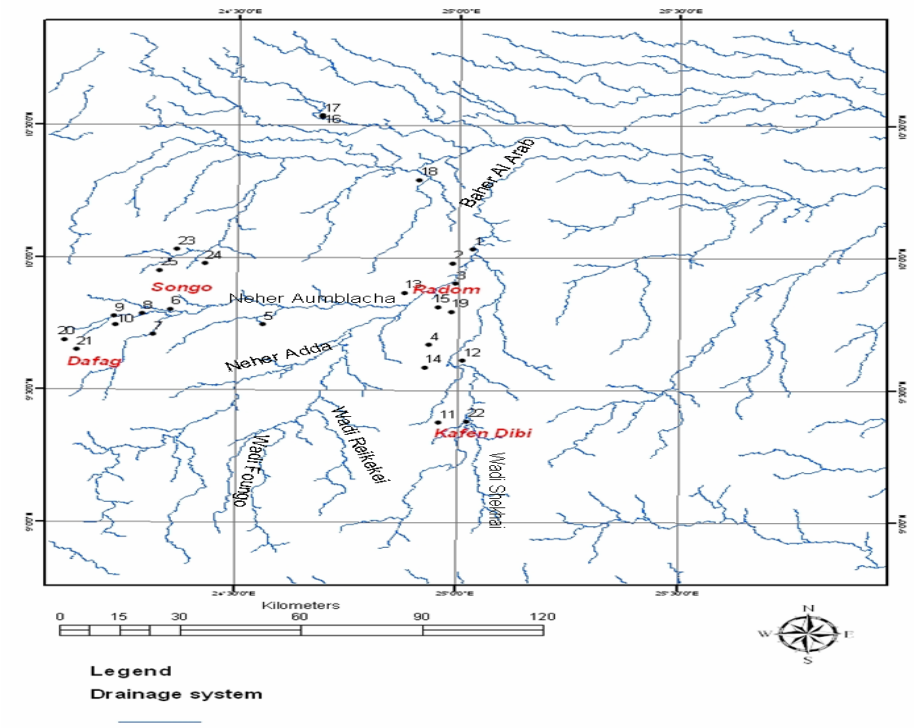

of the streams.

Fig (2) Drainage system of study area

3- Data Collection and Analysis

3.1 Collection of water samples: -

Water samples were collected from different sources including hand pumps wells, water yards, traditional dug wells, (masheish, gammam) and surface water, around Radom area between latitudes 8˚ 46́ 12.21N and 10˚ 53́ 15.56N longitude 24˚ 03́ 56.46E and 25˚ 59́ 10.17E Fig (2).

3.2 Determination of total hardness (TH)

EDTA titaramitric method: -

50 ml sample was placed into a 200 ml conical flask. PH was adjusted to 10 by gradually adding of buffer solution. About 0.03 – Erichrome black T was added to the solution. Then the solution was titrated against EDTA till the color changed from red to blue.

Calculation: -

$$\text{TH as CaCO3 mg /L} = \frac{\text{VX 0.01 M} \times 1000 \times \text{MWT}}{\text{ml of small}}$$

Where: -V = volume of EDTA from burette

0.01M = concentration of EDTA

MWT= molecular weight of CaCO3

3.3 Determination of calcium by EDTA tetrameter method.

50ml sample was placed in a 250 ml conical flask. The pH was adjusted by adding 2 ml of sodium hydroxide .0.1 mg of murexide indicator was added.The solution was then titrated against 0.01 M EDTA till the color was changed from violet to pink

V- Calculation: -

Ca mg/l = A× 40 × 0.01 × 100% ml sample.

Where (A) is the volume of EDTA from burette.

Estimation of magnesium

Mg mg/l = (TH mg/l – Ca mg /l)

3. 4-1-Determination of chloride ion by argentometric method

In 250 ml beaker a 50 ml sample was taken .1 ml of potassium chromate was added.The solution was titrated against silver nitrate 0.014 M till a pinkish yellow precipitate was produced distill water being used as a blank was titrated by the same method.

V-Calculation: -

$$\text{Cl mg /l} = \frac{(A - B)\ 35.45 \times o.1\ M \times 1000}{50\ \text{ml sample}}$$

Where: -

A = ml titrates for sample. B= ml titrates for blank. M = molarity of Ag NO3

3.5-Determination of bicarbonate

50 ml sample was taken into 25 ml conical flask.3 drops of methyl orange was added.The solution was titrated against sulfuric acid till the color of the solution was changed from violet to pink.

iV-Calculation: $\frac{-\ V \times 1000 \times 61\ (HCO_3\ MWT) \times 0.1\ ((H_2SO_4)\ con.}{50\ \text{ml sample}}$

Where: V = Volume of $H_2\ SO_4$

3.6 Determination of nitrate (NO3)

-Into a 25 ml cuvette 10 ml sample was taken.Nitrate reagent was added to the sample.The spectrophotometer was adjusted to zero by using 10 ml of a bank .The program was selected.The prepared sample was placed in spectrophotometer.The reading was taken from displayer. (A.P.H.A 1975).

iV-Calculation: - R×4.4=NO3 ppm

Where**:** R=Reading from the displayer**.**

2.7- Determination of sulfate anion: -

10 ml was taken into 25 ml Cuvette. Sulfaver 4 reagent was added. Adjusted to zero by using 10 ml of sample as blank.The program was selected. The prepared sample was putt in spectrometric (DR/2400). Reading was taken from the display (A.P.H.A1984)

V-Calculation: -

Sulphate ions can be Calculated directly.

4 - Results and discussion

4.1 -Descriptive statistic: -

A summery statistic of all measured parameters was present in table (1), for wets (A), dry seasons (B), illustrating the range, maximum, minimum, mean, variance, standard deviation, skew ness and kurtosis to each parameter.

Table (1) Summary of descriptive statistics of the measured hydro geochemical parameters in wet season (A) and dry season (B).

	N	Range	Minim	Maxim	Sum	Mean		Std.	Varian	Skewness		Kurtosis	
	Statistic	Statistic	Statistic	Statistic	Statistic	Statistic	Std. Error	Statistic	Statistic	Statistic	Std. Error	Statistic	Std. Error
pH	15	2.40	7.60	10.00	126.40	8.4267	.17416	.67450	.455	1.313	.580	1.328	1.121
EC	15	415.00	137.80	552.80	4425	295.0	33.1338	128.3	16468	.739	.580	-.494	1.121
TDS	15	290.50	96.46	386.96	3026	201.7	22.3799	86.68	7513	.968	.580	.166	1.121
Na	15	140.40	25.60	166.00	1241	82.70	8.53818	33.07	1094	.790	.580	2.142	1.121
Mg	15	38.67	1.89	40.56	106.39	7.0928	2.52502	9.779	95.636	3.291	.580	11.383	1.121
Ca	15	60.53	6.32	66.85	360.14	24.01	4.92607	19.08	364.0	.885	.580	-.095	1.121
k	15	12.84	.26	13.10	83.53	5.5687	1.12776	4.368	19.078	.215	.580	-1.388	1.121
Cl	15	64.65	5.75	70.40	322.01	21.47	4.24323	16.43	270.1	2.029	.580	5.178	1.121
SO4	15	8.00	1.00	9.00	63.20	4.2133	.70325	2.724	7.418	.581	.580	-.719	1.121
NO3	15	7.00	1.00	8.00	42.00	2.8000	.52735	2.042	4.171	1.530	.580	1.937	1.121
HCO3	15	199.82	2.68	202.50	1241	82.73	16.4435	63.69	4056	.243	.580	-1.120	1.121

(A)

	N	Range	Minim	Maxim	Sum	Mean		Std.	Varian	Skewness		Kurtosis	
	Statistic	Statistic	Statistic	Statistic	Statistic	Statistic	Std. Error	Statistic	Statistic	Statistic	Std. Error	Statistic	Std. Error
pH	25	1.50	7.30	8.80	203.60	8.1440	.0811	.40526	.164	-.409	.464	-.700	.902
EC	25	546.00	98.90	644.90	7436	297.5	33.10	165.5	27397	.544	.464	-.797	.902
TDS	25	388.23	63.20	451.43	4623	184.9	22.05	110.2	12150	.728	.464	-.326	.902
NA	25	162.67	12.00	174.67	1341	53.65	7.446	37.23	1386	1.626	.464	3.610	.902
Mg	25	50.20	2.82	53.02	437.85	17.51	2.752	13.76	189.4	.886	.464	.303	.902
Ca	25	72.00	4.90	76.90	596.71	23.87	3.522	17.61	310.1	1.355	.464	2.073	.902
K	25	12.73	.17	12.90	75.23	3.0092	.7749	3.875	15.012	1.270	.464	.345	.902
Cl	25	65.19	4.91	70.10	547.24	21.89	3.901	19.51	380.5	1.370	.464	.749	.902
SO4	25	25.50	.50	26.00	164.60	6.5841	1.325	6.626	43.898	1.311	.464	1.522	.902
NO3	25	126.27	.01	126.28	590.49	23.62	5.552	27.76	770.6	2.403	.464	7.161	.902
HCO3	25	562.86	10.54	573.40	3704	148.2	29.94	149.7	22412	1.401	.464	1.408	.902

(B)

4.2. -Normality test: -

To apply any statistical test the data must be distributed normally. The normality of the data was tested by using a histogram for each parameter, employing Statistical Package for Social Science (SPSS). The test has shown that the data are not distributed normally(skewed) except TDS, TH and NO2 in wet season, and EC, and PH in dry season, this skewness in the analyzed data was confirmed by using square root, logarithm and sin transformations, so as to transfer the data to normal distribution (Rossiter,2006).

4.3-Nonparametric Correlations: -

Because most of the data is not normally distributed, simple we used nonparametric correlation method such, as Kendall's correlation coefficient has been calculated. The strength of relationships between two variables and whether one variable increases as the other decreases or the opposite is gauged by correlation coefficient (r). If r>0.75 the variables are classified strongly correlated and those variables with r›0.6-0.75 are moderately correlated, (Roossiter,2006). Also, partial correlation was used to depict the relationships between major cations and anions. Table (3) for wet (A) dry (B) seasons for partial correlation.

Table (3) Kendall's correlation matrix (A) wet season (B) dry season

	pH	EC	TDS	Na	Mg	Ca	Cl	SO4	HCO3
pH	1.000	.414*	.414*	.287	.059	-.039	.010	.237	-.287
EC		1.000	.962**	.249	.105	-.181	.115	.378	-.383*
TDS			1.000	.211	.143	-.219	.134	.378	-.421*
Na				1.000	.459*	.153	-.029	.230	.067
Mg					1.000	-.048	.000	.040	.096
Ca						1.000	-.115	-.279	.268
Cl							1.000	.130	-.048
SO4								1.000	-.340
HCO3									1.000

*. Correlation is significant at the 0.05 level (2-tailed).

**. Correlation is significant at the 0.01 level (2-tailed).

(A)

	pH	EC	TDS	NA	Mg	Ca	Cl	SO4	HCO3
pH	1.000	-.176	-.155	-.162	.079	.297*	-.177	-.152	.225
EC		1.000	.813**	.507**	.113	.050	.101	.097	.254
TDS			1.000	.507**	.127	.050	.114	.097	.254
NA				1.000	-.007	.010	.074	-.178	.161
Mg					1.000	.524**	.121	-.017	.455**
Ca						1.000	-.024	-.255	.365*
Cl							1.000	.145	-.081
SO4								1.000	-.151
HCO									1.000

*. Correlation is significant at the 0.05 level (2-tailed).

**. Correlation is significant at the 0.01 level (2-tailed).

(B)

4.4-Interrelation between the measured parameters

The relationships between the measured hydro chemical parameters shown in table (3 A&B) may lead to interpretation of the main processes contributing to the groundwater salinization. Moderate to strong correlation coefficients (r=0.507, 0.813, 0.507) between Na-EC, Na-TDS and EC-TDS indicate that the ground water was affected by factor of salinization. Moderate correlation coefficients (r=0.459, 0.524) between Na-Mg and Ca-Mg in the two seasons indicated that the groundwater samples were affected by cation exchange process. The moderate correlation coefficients(r=0.455,0.365) between Mg-HCO3 and Ca-HCO3 were found, which means that HCO3 and Ca are dominant or cations are indiscriminate, with Mg dominant or Ca and Mg. Important indicates, are often associated with dolomites, Ca Mg $(CO_3)_2$.

In partial correlation matrix, (table 4.), (A) wet season (B) dry season lack no anion or cation dominance, indicates that water exhibits simple dissolution or mixing.

Moderate correlation coefficient between Na and HCO3 indicates the appearance of thermonatrite Na2CO3.H2O in under saturation state. This means that the water samples are potential to dissolve this mineral.

Table (4). Partial correlation matrix (A) wet season (B) dry season

	Na	Mg	Ca	Cl	SO4	HCO3
Na	1.000	.350	.166	-.096	-.332	.542
Mg		1.000	.475	.250	-.010	.724
Ca			1.000	.026	-.223	.401
Cl				1.000	.031	-.052
SO4					1.000	-.255
HCO3						1.000

(A)

	Na	Mg	Ca	Cl	SO4	HCO3
Na	1.000	.324	.301	.039	.269	.350
Mg		1.000	.209	.012	-.220	.454
Ca			1.000	.394	-.376	.528
Cl				1.000	.082	.015
SO4					1.000	-.361
HCO3						1.000

(B)

4.5-Factor analysis

Factor analysis is a statistical technique that reduces the number of variables and detects structure in the relationships between these variables and classifies them (Davis, 2002).

In order to interpret the three groups of clusters the principal component in factor analysis is used. By using variance-maximizing (varimax) analysis, total variance values were shown in table (5) for the two seasons, wet(A) and dry (B).

Table (5) Showing total variance explained (A) wet season (B) dry season

	Initial Eigenvalues			Rotation Sums of Squared Loadings		
Component	Total	% of Variance	Cumulative %	Total	% of Variance	Cumulative %
1	3.703	41.144	41.144	3.390	37.661	37.661
2	1.704	18.936	60.080	1.776	19.736	57.397
3	1.151	12.786	72.866	1.392	15.469	72.866
4	.895	9.943	82.810			
5	.633	7.033	95.063			
6	.470	5.220	98.174			
7	.280	3.111	98.174			
8	.157	1.749	99.923			
9	6.899E-03	7.666E-02	100.000			

Extraction Method: Principal Component Analysis.

(A)

Component	Initial Eigenvalues			Rotation Sums of Squared Loadings		
	Total	% of Variance	Cumulative %	Total	% of Variance	Cumulative %
1	4.435	49.272	49.272	4.392	48.797	48.797
2	1.992	22.135	71.408	1.987	22.078	70.875
3	1.155	12.830	84.237	1.203	13.362	84.237
4	.697	7.743	91.981			
5	.348	3.868	95.849			
6	.202	2.241	98.090			
7	.126	1.397	99.487			
8	3.858E-02	.429	99.915			
9	7.632E-03	8.480E-02	100.000			

Extraction Method: Principal Component Analysis.

(B)

From table (5) which shows wet season data(A), the first component or factor explains 37.66 % of data variance. It's influenced by contribution of electrical conductivity, total dissolved solids, sodium and sulphate. This is also attributed to factor of salinization in ground water. Sodium, magnesium and bicarbonate form the second principle component .This factor may be related to ion- exchanged waters although generation of CO2 at depth can produce HCO3 where Na is dominant under certain circumstances (Winoggard and Farlekas 1974). This explains the 19.73% of data variance.

The third principal component, which explains 15.46%, is contributed by calcium and chloride that may be due to the ground water mineralization that appears in reverse ion exchangeable process.

From table (4) (B) dry season first component or factor explains 48.79% of data variance, contributed by electrical conductivity, total dissolved solids, sodium, calcium, magnesium and bicarbonate, this is due to factor of salinization also may be related to dissolution of Ca and Mg bearing minerals (calcite, dolomite minerals).

The second factor explains 22.1% of data variance that contributed by pH, NO dominant anion or cation, indicates waters that exhibit simple dissolution or mixing.

The third factor component contributed by chloride and explains 13.36% of data variance which is due to the ground water mineralization; which may result from reverse ion exchange of Na-Cl.

4.6-Test of seasonal variations: -

The groundwater samples in the study area were collected in two seasons so it necessary to check the coefficient difference between the two seasons, to assess this Mann-Whitney U test (Roossiter, 2006) was performed. Mann-Whitney U test. is the most popular of the two-independent-samples tests. It is equivalent to the Wilcoxon rank sum test and the Kruskal-Wallis's test for two groups.

From table (6) it is noticed that there is no significant difference between all parameters in the two seasons, except for Na, Mg this implies that the two sampled populations were equivalent in location.

Table (6) Mann-Whitney Test for significant difference

	pH	EC	TDS	Na	Mg	Ca	Cl	SO4	HCO3
Asymp. Sig. (2-tailed)	.361	.856	.459	.005	.004	.878	.530	.780	.288

5- Conclusions and Recommendation

5.1-Conclusions: -

1- A summary of descriptive statistics of all measured parameters in the wet and dry seasons showed that the dominant cation is sodium followed by calcium and magnesium. While potassium is minor. Bicarbonate is the dominant anion followed by chloride and Sulphide.

2- The measured parameters have shown, moderate to strong correlation between magnesium, calcium and bicarbonate, indicating dominance of dolomite and carbonate rocks as, water acts as weak carbonic acid leading to soluble carbonate constituents. The cationic composition of the water is calcic due to leaching of alkali elements in carbonate constituents, which easily go to solution by solubility.

3- Moderate to strong correlation between sodium, electrical conductivity, and total dissolved solids such correlation is normal since these parameters are the main factor that control salinity of water.

4- Partial correlation showing that no dominant anion, no dominant cation, that means the water exhibiting simple dissolution or mixing processes

5- Moderate correlation between sodium and bicarbonate is indicated due to the presence of Thermonatrite Na_2CO_3: H_2O and halite NaCl in under saturated state in the calculated of saturated indices.

6- No seasonal variations between (concentrations) most of the parameters due to seasonal renewal of ground water storages in fracture zones by recharge.

References: -

1- (A.P.H.A 1975). **American Public Health Association,"** Standard methods for the e xamination of Water - Waste Water," 14th Ed. A.P.H.A., A.W.W.A. and W.P.C.F. Washington D.C. **(1975).**

2-(A.P.H. A1984) **American Public Health Association,** Standard methods for the examination of Water - Waste Water, 17th Ed. A.P.H.A., A.W.W.A., And W.P.C.F.,Washington D.C. .**(1984**)

3-**. (**Armand, 1965). **Armand.Louis."** Water treatment-Hand Book "Stephen Austin &Sons Ltd, Caxton Hill, (1965). Great Britain.

4- **(**. (Bsnraju, 1995). **BSNRAJU, "**Water supply and wastewater engineering "Tata McGraw- Publishing Company Limited **(1995).** NEW DELHI

6-(Davis, 2002). **Davis, J.G**." Statistics and data analysis in geology," John Wiley & Sons. Inc., NY. **(2002**)

7-(Nason, 1965). **NASONALVIN."** Modern Biology",HarperCollinnsPublishers INC, NEW YORK**. (1965)**

8- (Rossiter,2006). **D.G.Rossiter**.,"An Introduction to statistical analysis overheads"Department of Earth systems Analysis-International instude for Geo-information sciences earth observation (ITC). **(2006).**

1. يعقوب اسحق أبو الزاكى، رسالة دكتوراه –حوض وأدى إبرة –دراسة جيومورفولوجية-جنوب دارفور-جامعة النيلين. 2003م.

ISSN (Print): 2958-8987
ISSN (Online): 2958-8995
Doi: 10.59799/APPP6605

Depth Prevalence of Petroleum Residue in Different Soil Texture

Baraa Mohammed Ibrahim Al-Hilali

Biology Department, College of Education, University of Samarra.

Email: barabio86@gmail.com

Abstract

The results recorded the highest prevalence of residues at 218.5 ppm in mixed soils, while the lowest prevalence in mud soils was 44.8 ppm; The highest electrical conductivity in mixed soil was 5.37 micro centimeters/cm and the lowest electrical conductivity was 1.81 micro centimeters/cm; When measuring the sand function, the sand soil recorded 8.3 while the gypsy soil recorded 7.5; When the relative moisture in the soil was measured, the mixed soil recorded the highest rate of 93.55%, while the lowest moisture in the gypsy soil recorded 57.90%; When the heavy elements (cobalt, cadmium and lead) were measured, the higher readings were as follows (15.40 per sand, 58.10 per gypsy, 122.80 per mix) and the lower readings were as follows (7.10 per clay, 14.60 per clay, 71.90 per clay) respectively.

Keywords: Prevalence, Petroleum Residue, Soil Texture, Depth.

Introduction

Soil pollution results mainly from man's inability to deal efficiently and safely with air and soil pollution, water sources and waste disposal resulting from his human and industrial effectiveness the most important aspect of soil pollution is the methods of discharging solid and semi-solid waste, the presence of hazardous chemicals in the environment and the deformation of the soil's surface, Chemical contamination is one of the most dangerous and endangering contaminants because chemicals can enter natural life cycles and thus affect food, health and the perpetuation of human existence (Adam, 1988), animal and plant

In addition, it is the role of running water carrying the contaminants it creates for the soil when it comes into contact, because the movement of water pushes the contaminants towards the surface, thus depositing the contaminants in the soil and the degree of risk of many pollutants depends on the composition and concentration of the contaminated substance, as indicated by (Abayji, 1988) refers to the spread and distribution of contaminants between water, air, land and living, and their focus depends on the image of the contaminant, such as being dissolved or stuck in water, or glued to dust minutes, in either case these contaminants are deposited in the soil by either falling or deposition.

Heavy total petroleum hydrocarbons are the most harmful pollutants for their direct and indirect impact on the growth of plant organisms, animals and other biota and, on the other hand, crude oil, its derivatives and

manufactured hydrocarbons are among the most important environmental pollutants being toxic to most organisms. as well as carcinogenic and transmissible in food chains, in addition to their complex composition and large molecular size, the importance of the treatment of hydrocarbons contaminated by the environment is demonstrated as the most important objective for avoiding damage to the biosphere, which extends to most organisms, including humans (Nasr, 2000).

The oil industry is also one of Iraq's most important and important industries for the national economy. However, this industry has caused high levels of land, water and air pollution and has caused a clear ruin in the use of these sources (Hanoush, 2004).

The study aimed to identify the oil pollutant's susceptibility to various types of soils and its ability to transmit through soil types and its potential to contaminate groundwater, and to try to select the best types of soils that prevent the liquid pollutant from leaking to be used as sanitary disinfectants for many wastes.

Materials & Methods

The research included a study of the prevalence of oil residues in segments of four different tissues, namely soil (sand, gypsy, blend, mud), which was conducted using a box made of non-waterproof wood; Divided into four segments with boiled-tin wooden barriers to ensure that oil waste does not spread among different types of soils, a central perforated and boiled-tin jar was left with a container made of filtration paper. The container was filled with petroleum waste, which is allowed to leak into the four soil segments through the holes, where the oil waste was allowed to spread for 45 days, after which a series of analyses were conducted to search for the oil waste in the segments of the experience soil

Volume Distribution and Composition of Soil

The experiment was conducted based on the hydrometer method mentioned (FAO, 1974).

PH acidic function

Using a hydrogen exponentiator. (McLean, 1982) used the method he mentioned

EC Electrical Connectivity

and using an electrical conductivity measurement device. Richards, 1954 has used a method (

Humidity Relative humidity

The assessment of soil content of water (moisture) for air-dried samples was performed in the laboratory by (Hesse, 1971) Using a relative humidity measurement device.

Soil Content of Oil

The content of the soil was measured according to the method mentioned (Chaineau et al., 2003).

ble 1: Physical and chemical properties of Kirkuk crude oil medium used in the study

NORTH REFINERIES COMPANY (GENERAL CO.)
LABORATORIES DEPARMENT
FINAL PRODUCTS EVALUATION SECTION
COMPUTERIZED PRODUCTS CERTIFICATE
(NR. SR2.SR1)

SOURCE: KIRKUK CRUDE OIL
DATE: 1ST . TO 30 November /2010
AVERAGE RESULTS

ITEM	TEST		UNIT	AVERAGE	SPECIFICATION
1.	SP. GRAVITY @15.6 C°		--	0.8492	0.8559-0.8443
2.	A.P.I GRAVITY		----	35.1	34-36
3.	R.V.P @ 37.8 C°		PSI	5.8	
4.	SALT CONTENT		Mg/L	10.5	30 MAX
5.	VISCOSITY @ 37.8 C°		CST	4.5	
6.	VISCOSITY @ 50.0 C°		CST	3.4	
7.	POUR POINT C°		DEG	-32	
8.	B.S & W CONTENT		VOL %	Trace	0.15 MAX
9.	CARBON RESIDUE (RAMS)		WT %	3.6	
10.	H_2S CONTENT		PPM	10.7	30 MAX
11.	TOTAL SULPHUR CONTENT		WT %	2.4	
12.	ASH CONTENT		WT %	0.009	
13.	ASPHALTENE		WT %	0.82	
14.	VANADIUM		PPM	33.0	
15.	NICKEL		PPM	12.0	
16.	ASTM DISTILLATION I.B.P		DEG	41	
	RECOVERY AT	50 C°	VOL %	1.7	
		75 C°	VOL %	6.7	
		100 C°	VOL %	10.7	
		125 C°	VOL %	13.8	
		150 C°	VOL %	25.4	
		175 C°	VOL %	26.6	
		200 C°	VOL %	31.0	
		225 C°	VOL %	33.6	
		250 C°	VOL %	38.4	
		275 C°	VOL %	42.6	
		300 C°	VOL %	48.3	
	TOTAL DISTILATE		VOL %	51.0	
	TOTAL RESIDUE		VOL %	48.0	

CHEMIST IN CHARGE

DEPT.MANAGE
حسام يوسف ياسين

Table 2: Chemical Ingredients for Kirkuk Crude Oil Medium Used in Study

Elements	Percentage
Carbon	%86
Hydrogen	%11
Sulfur	%2.1
Nitrogen	%0.05
Vanadium	%0.0025
Nickle	%0.0015
Sodium	%0.0020
Potassium	%0.0006
Calcium	%0.0021

Table 3: Soil Texture

Texture| Soil Type	Sandy Soil	Silty-Clay Soil
Sand	%50	%32
Clay	%32	%30
Silt	%18	%38

Table 4: pH Acidity function in soils before and after treatment with crude oil

Soil Type	Soil Depth					
	15 cm		30 cm		45 cm	
	After Crude Oil	Control	After Crude Oil	Control	After Crude Oil	Control
Sandy Soil	8.20	8.27	8.10	8.27	8.15	8.27
Silty-Clay	7.57	7.87	7.55	7.87	7.52	7.87

The results were indicated in table 4 of the acidic function measured in two types of soil (sand and mix). The results showed the highest rate at all depths in the untreated sand soil at 8.27, while the lowest at all depths in the clay soil at 7.87; The cause of oil pollution was a moral reduction of 15cm deep in the mixed soil, which was 7.52. On the other hand, the distance from the pollution center showed moral differences in the sour function, with the highest function rate in the sand soil in the 60cm dimension, at 8.30, while the lowest function rate in the mixed soil in the 30cm dimension, at 7.60.

The decrease and decrease in the acid function is explained by the oil's containment of sulfur and some halogens and chlorides with acid effect on the medium in which it is present. The base of the medium decreases and its acidity increases (Hamid and Kamel, 1998).

Table 5: EC Electrical conductivity before and after treatment with crude oil

Soil Type	Soil Depth					
	15 cm		30 cm		45 cm	
	After Crude Oil	Control	After Crude Oil	Control	After Crude Oil	Control
Sandy Soil	3.09	3.24	3.09	3.24	3.09	3.25
Silty-Clay	5.93	7.38	6.66	7.38	6.65	7.38

The results were shown in table 5, the electrical connectivity in the soil types used in the study (sand and mix) prior to the treatment of crude oil. The results showed that the highest conductivity rate occurred in the mixed soil and in all depths, at 7.38 micro-smins, while the lowest delivery rate was in the sandy soil and at all depths, at 3.24 micro-smins; The cause of oil contamination is a moral reduction in connectivity of 3.09 at all depths.

On the other hand, the distance from the pollution center showed moral differences in connectivity, with the highest conductivity rate being 7.79 micro-smins in the 30cm dimension, while the lowest connectivity rate was 3.11 micro-smins in the 120cm dimension.

In general, electrical conductivity decreases with the low concentration of electrolytes due to the phenomenon of expansion and dispersion that are affected by the type of positive ions present in the soil (Dograma G, 1990).

Table 6: Relative moisture rate in soils before and after treatment with crude oil

Soil Type	Soil Depth		
	15 cm	30 cm	45 cm

	After Crude Oil	Control	After Crude Oil	Control	After Crude Oil	Control
Sandy Soil	50.63	76.46	50.65	74.21	50.65	74.21
Silty-Clay	63.07	93.55	63.00	93.55	63.05	93.55

The results in table 6 show the relative humidity rate in two types of soil The results showed that the highest relative humidity rate was in the mixed soil and at all depths, at 93.55%. While the lowest humidity rate in sand soil and deep soil was 30cm and 60cm, it was 74.21% Soil contamination with crude oil caused a moral reduction of the humidity rate, the most severe in the 45cm deep sandy soil, at 50.63%.

The gradual decrease in relative humidity in soil segments taken by oil molecules to replace water molecules and evaporation of water molecules can be explained by the fact that soil molecules are associated with oil molecules with a stronger bond than soil particles with water due to the presence of magnesium, calcium and some high surface tensile organic compounds (Ramadan and his group, 1991).

Table 7: Pb Concentration in soils before and after treatment with crude oil

Soil Type	Soil Depth					
	15 cm		30 cm		45 cm	
	After Crude Oil	Control	After Crude Oil	Control	After Crude Oil	Control
Sandy Soil	109.57 b	109.65 a	109.55 b	109.55 b	109.47 b	109.40 c
Silty-Clay	a122.65	a122.85	122.65 a	a122.85	122.77 a	a122.90

Results in Table 7 showed lead concentration in two types of soil (sand and mix) prior to the treatment of crude oil, showing that the highest concentration of lead was in mixed soil with 122.82 ppm in depth of 15cm, while the lowest concentration of lead in sand soil 109.40 in depth of 15cm, caused the soil to be contaminated with oil with a moral reduction of 109.00 ppm.

The values of the concentration of lead in the soil varied from the distance closest to the pollution center and gradually increased towards the distance away from the pollution center due to the carrying of the liquid to the element from the place of flow to the place farther, which was interpreted. S. F. D. A) This case is the FDA in an article published in 2010

Table (8) Cobalt concentration in soils before and after treatment with crude oil

Soil Type	Depth Soil					
	15 cm		30 cm		45 cm	
	After Crude Oil	Control	After Crude Oil	Control	After Crude Oil	Control
Sandy Soil	15.40 a	15.37 a	15.40 a	15.36 a	15.35 a	15.35 a
Silty-Clay	11.77 a	11.77 a	11.75 a	11.75 a	11.77 a	11.77 a

The results in table 8 show the concentration of cobalt in the types of sand and mixed soils, with 15.37 ppm the highest cobalt concentration rate in sand soils and 45cm deep, 11.77 ppm the lowest in mixed soils and at 15cm and 45cm, there are no moral differences in cobalt concentration after treatment with crude oil. There was also no moral difference in distancing from the pollution center, with the highest cobalt concentration rate being 15.41 ppm in dimensions 90cm and 120cm in sandy soil.

Table 9: cadmium Concentration in Soils Before and After Treatment with Crude Oil

Soil Type	Depth Soil					
	15 cm		30 cm		45 cm	
	After Crude Oil	Control	After Crude Oil	Control	After Crude Oil	Control
Sandy Soil	47.20 a	47.20 a	47.17 a	47.17 a	47.20 a	47.12 a
Silty-Clay	25.25 a	25.25 a	25.27 a	25.27 a	25.17 a	25.17 a

The results in the table show 9 the concentration of cadmium in the sand and mix soil types, with 47.20 ppm the highest cadmium concentration rate in the sand soil and at depth 45cm, and the lowest 25.17 ppm in mixed soil and at depth 15cm, there are no moral differences in the concentration of chromium after treatment with crude oil. There was also no moral difference in the distance from the pollution center, with the highest chromium concentration rate being 47.31 ppm in the 120cm dimension.

Table 10: Average of Oil Residue Diffusion in Soil Depth

Soil Type	Silty-Clay			Sandy Soil		
Soil Depth	15 cm	30 cm	45 cm	15 cm	30 cm	45 cm
Concentration	218,5	203.9	185.3	0	0	128.2

Results in table 10 show the prevalence of oil residues in two types of soil The results indicated that the highest prevalence rate occurred in mixed soils, with 218.50 parts of a millionth depth of 15 centimeters, followed by the same 30cm deep soil, with a prevalence rate of 203.91 parts of a millionth, While the lowest prevalence of oil waste in sandy soil was 15cm and 30cm, there was no spread which is due to the nature of the soil, where the sandy soil has very high interstitial spaces and has relatively large grain size, allowing all liquids to access the bottom, i.e. they cannot retain the means because of the large size of the intersection distance, For mixed soils, the highest prevalence is due to their ability to retain liquids for longer. This in turn is due to small interreligious distances and the inclusion of this type of soil in mud grains, which they started to interact with oil residues because they possess effective mineral elements that have the ability to interact with oil (Dougramji, 1990).

References

– Lead Co- Al-Abayji, Jamal Kamel. 1988. The role of the Shatt al-Arab River as a carrier of pollutants to the Persian Gulf. Publications of the Marine Science Center (9), University of Basra. p.: 25-34.

-Al-Nuaimi, Saadallah Najm Abdullah. 1999. Fertilizers and Soil Fertility. Dar Al-Kutub for Printing and Publishing, Mosul, Iraq.

-Hannoush, Ali Hussein Aziz. 2004. The Iraqi Environment, Problems and Prospects. Iraqi Ministry of Environment.

-Dograma J, Jamal Sherif. 1990. Introduction to Soil Physics. Translator. Baghdad University.

-Ramadan, Omar Musa. Al-Ghannam, Khaled Ahmed Abdullah. Thanoun, Ahmed Abdel Karim. 1991. Industrial Chemistry and Industrial Pollution. Dar Al-Hikma for Publishing and Distribution, Mosul.

- Issam Hamid and Nael Kamel, 1998. The effect of oil derivatives on facilities. Edited by Al-Harbi, Muwaffaq Jassem. National Center for Construction Laboratories - Directorate of Research and Technical Affairs.

-Nasr, Raed Bahr. Bacteriological and genetic study of bacteria that consume hydrocarbons. Master's Thesis, College of Science - University of Baghdad.

- Adam. G.A. (Translator). “Environmental pollution”, Basrah University Press, 1988.

- Chaineau, C. H.; Yepremian, C.; Vidalie, J. F.; Ducreux, J. and Ballerini, D. (2003). Bioremediation of a crude oil – polluted soil: Biodegradation, leaching and toxicity assessments. Water, air and soil pollution an international journal of environmental pollution, Vol. 144, No. 1 – 4, PP: 419 – 440.

- FAO. 1974. The Euphrates Pilot Irrigation Project. Methods of Soil Analysis, Gadeb Soil laboratory (A Laboratory Manual). Food and Agriculture Organization, Rome, Italy.

- Hesse, P. R. 1971. A Textbook of Soil Chemical Analysis. John Murray, London.

- McLean, E. O. 1982. Soil pH and Lime Requirement. P. 472-506. In A. L. Page(ed.), Methods of Soil Analysis, Part 2: Chemical and Microbiological Properties. Am. Soc. Agron., Madison, WI, USA.

- Richards, L. A. 1954. Diagnosis and Improvement of Salin and Alkali Soils. USDA Agric. Handbook 60. Washington, D. C.

-U. S. F. D. A;(2010). Import and Domestic ntamination. U. S. Food and Drug Administration. CPG Sec. 545-550.

Physics and Procedure of Gamma knife Radiosurgery

Assis. Techer. Alyaa Hussein Ashour[1, a]

[1]*University of Mashreq, Baghdad, Iraq*
[a)] Alyaa.hussein.a@uom.edu.iq

Abstract

GKRS, developed by Lars Leksell and Borje Larsson, is a kind of radiosurgery that employs numerous gamma radiation beams from Cobalt-60 sources to converge on a single focus point known as an isocenter. To match the patient to a physical coordinate system, stereotaxic is performed utilizing a stereotactic head frame for GKRS. The Gamma Knife Radiosurgery System (GKRS) is the gold standard for stereotactic radiosurgery to the brain, and the Perfexion is a new variant of the Gamma Knife specially created for the radiosurgical treatment of numerous metastases.

The first gamma unit required a significant leap of faith. No such machine existed, nor had any machine ever been developed for the purposes for which this machine was designed. At a time when stereotaxy was not widely acknowledged by neurosurgeon peers, the suggested apparatus was designed to treat a limited number of patients using a stereotactic technique. The Swedish government wanted large amounts of data in order to develop and practice radiosurgery, but no financial help was offered. This was gained privately.

Keywords. Gamma Knife, Radiosurgery, GKRS, Radiation Dose.

1. Introduction

The Leksell Gamma Knife is a highly sophisticated therapy unit that employs a stereotactic approach to the treatment of brain tumors, vascular abnormalities, and pain problems. Inside the protected treatment unit (see Figure 1), beams from 201 Co-60 radioactive sources are focused such that they meet at the same place in space. As a result, a spherical zone of a high dose is created, known as a shot of radiation. By mixing various doses of radiation, the treatment technique may be adjusted to target lesions of varied sizes and forms. [1]

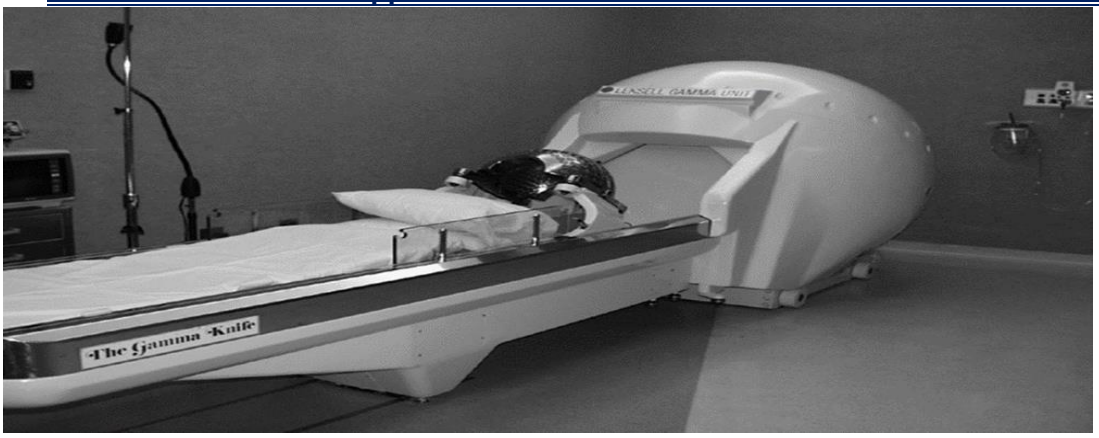

Figure (1): Gamma Knife Treatment Unit

2. Gamma Knife history

Leksell released landmark research on radiosurgery in 1951, which was a declaration of principles that were all remarkably well-known at the time. The initial cases treated with a commercially available industrial X-ray machine attached to the Leksell arc and frame were effective enough to motivate more attempts to improve the method. In 1953, the arc of the stereotactic device was coupled to an orthovoltage X-ray tube, and Leksell tested his idea by treating two patients with trigeminal neuralgia using SRS. (See figure 2).[2]

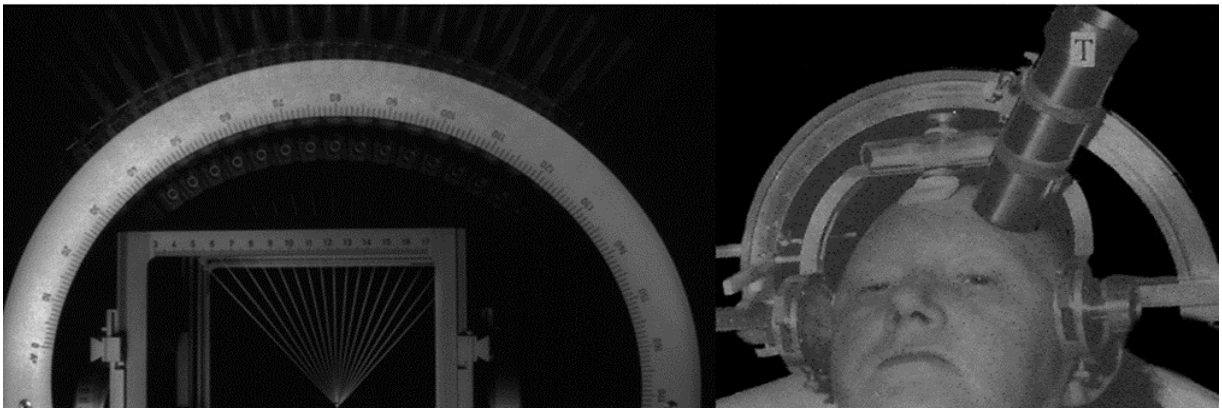

Figure (2): The first patient treated by connecting the stereotactic arc to an orthovoltage X-ray tube.

In the late 1950s, Leksell met Börje Larsson, a radiobiologist, and physicist who would become the head of the Gustav Werner synchrocyclotron lab in Uppsala, about an hour north of Stockholm. Leksell was the chairman of neurosurgery at Lund at the time. They began a comprehensive investigation into the future prospects of Leksell's non-invasive alternative to open brain surgery. [2]

Later, Leksell and physicist Börje Larsson utilized rabbits and goats in radiobiology experiments to determine and quantify the effects of focused fine beam radiation on the brain. The goal was to destroy the normal brain in order to cure functional brain illness using focused radiation. There was umbrage with proton radiosurgery, and it became widely believed in Sweden that proton beam radiosurgery was overly complicated and impractical. It was clear that a new machine was required. It would have a fixed design. Complex collimators were created to create beams with acceptable properties when powered by Co-60 sources. The machine's geometry was calculated, which included the distance of the sources from the patient and the optimal distance between the sources. [3]

The first Gamma Knife was installed in 1968, and over the next 50 years, Gamma Knife surgery has expanded to include much of what is done in neurosurgery, with over 330 Gamma Knife clinics throughout the world. More than 1.2 million people had received Gamma Knife surgery by the end of 2017. [2] Finally, the first patients were treated in Uppsala in 1961. (Figure 3)

Figure (3): The first patient treated with the synchrocyclotron in Uppsala.

3. The Evolution of Gamma Knife Technology

Since its inception in 1967, the Gamma Knife has undergone various modifications.

Model A (or U), 201 Cobalt sources were grouped in a hemispheric shape in the initial versions, these devices faced difficult Cobalt-60 loading and reloading challenges. To remove this issue, the unit was reconfigured so that the sources were grouped in a circular (O-ring) arranging (models B, C, and 4C), see figure (4). [4]

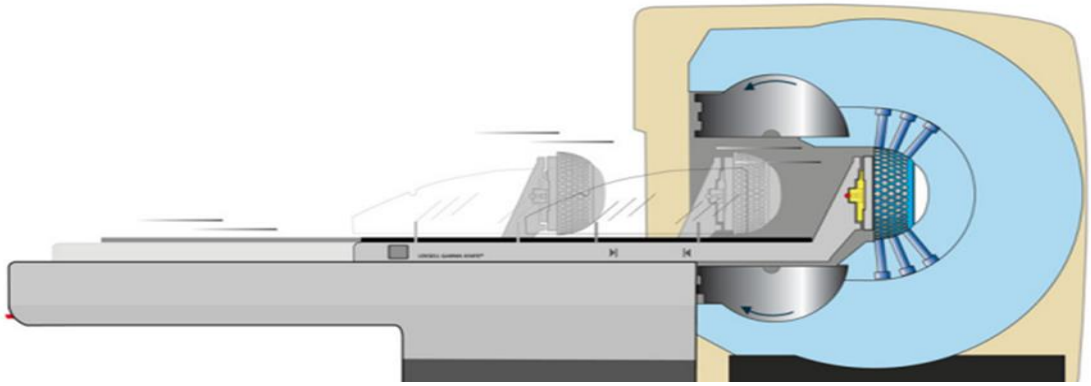

Figure (4): Schematic diagram of model 4C Gamma Knife unit (Courtesy of Elekta AB, Stockholm, Sweden.)

Gamma Knife design was created in 1999. In March 2000, the University of Pittsburgh Medical Center became the first in the United States to install a Model C. This method combines advancements in dose planning with robotic engineering and employs an autonomous positioning system with submillimeter accuracy (APS) see figure (5). This technology (APS) eliminates the requirement for each set of coordinates in multiple isocenter designs to be manually adjusted. The robotic positioning device moves the patient's head to the treatment plan's target coordinates.

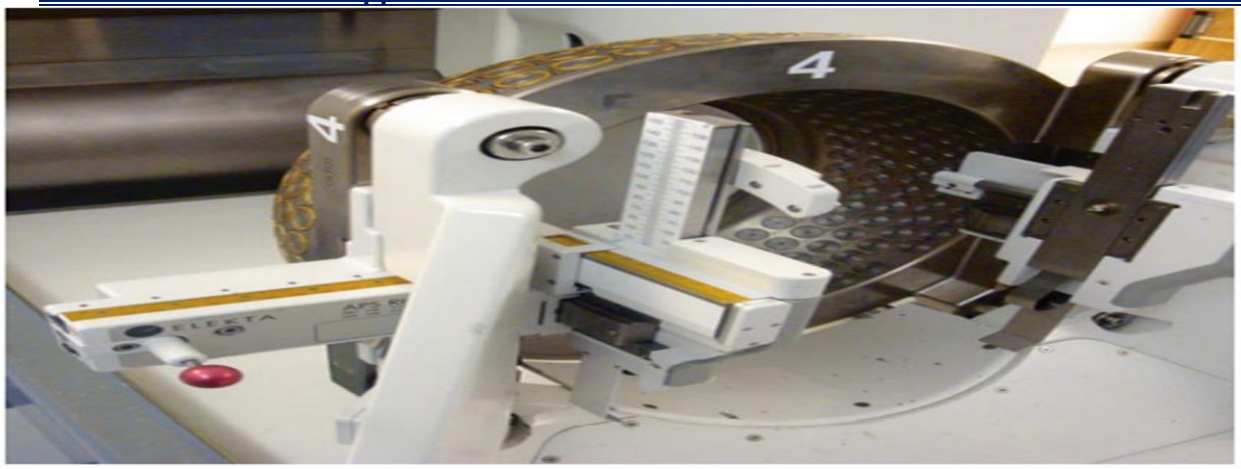

Figure (5): Gamma Knife 4C automatic positioning system.

The model 4-C includes innovations that are intended to improve workflow, boost accuracy, and give integrated imaging capabilities. The integrated imaging, enabled by Leksell Gamma Plan, provides for the merging of images from multiple sources. The planning information is available by both sides of the treatment couch. The helmet changer and robotic APS are faster and decrease total treatment time see figure (6), and Gamma Knife PERFEXION module is the most recent implementation of this technology.[5]

Figure (6): Gamma Knife 4C unit (Courtesy of the University of Pittsburgh Gamma Knife Facility, 2013.)

3.1 Gamma Knife Perfexion

Because of the considerably different geometry of this device compared to prior Gamma Knife versions, it was carefully evaluated before being put into commercial usage. It certainly makes the use of the Gamma Knife faster and more efficient for the user, while also allowing access to any area within the cranium and making the process more comfortable for the patient. [6]

The Perfexion TM (PFX) unit is made up of 192 sources that are separated into eight distinct sectors or radiation source banks see Figure (7). Each sector can be robotically driven to deliver beams with diameters of 4 mm, 8 mm, or 16 mm, or no beam at all. The automated features of PFX have eliminated the requirement for human helmet changes, which were required in LGK previously models. [7]

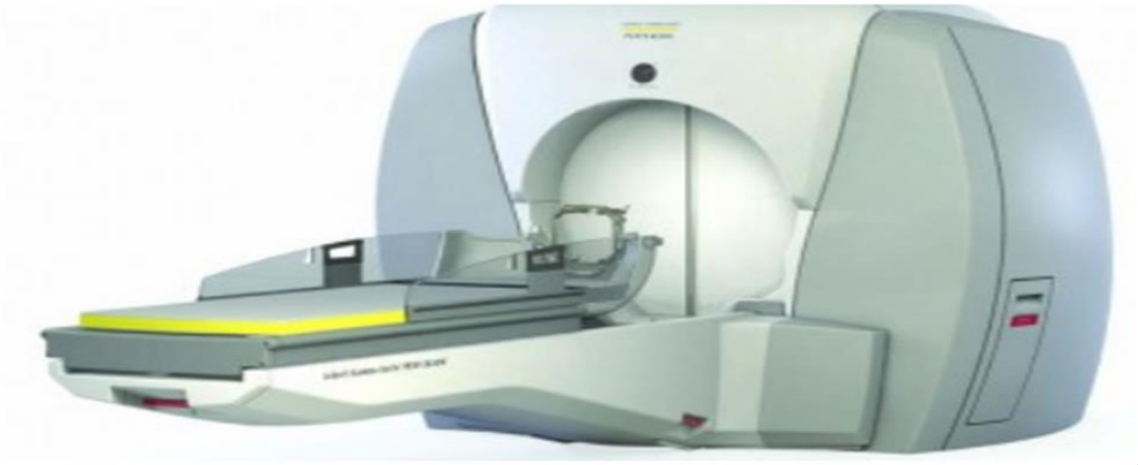

Figure (7): The Leksell Gamma Knife Perfexion

Beginning in 2002, the manufacturer asked an invited group of neurosurgeons, radiologists, and medical physicists to design specifications for a new Leksell Gamma Knife system. The group made an agreement on five important features for a new system:

1) Best dosimetry efficiency.

2) Unlimited cranial connect.

3) Better radiation coverage for patient and apparatus.

4) Full automate of the therapy.

5) Patient and staff safety.

6) Same dosimetry for the smaller collimator as previous units.

In 2006, the new unit was first installed in Marseille, France. The Perfexion system was installed and completed in Prague, Czech Republic, in 2009. [8]

That has 192 CO-60 sources dispersed in 8 cylindrically organized sectors. Each sector has 24 sources distributed across five rows, which when aligned with the adjacent sectors generate five rings of beams. The radiation beams are formed using collimators, which are cylindrical 120 mm long tungsten tubes integrated into a collimator body.

Three collimator sizes, 4, 8, and 16 mm, are included, and an automatic drive mechanism moves each sector back and forth, allowing selective exposure of the collimators of the chosen size to the sources (Fig 8).[9]

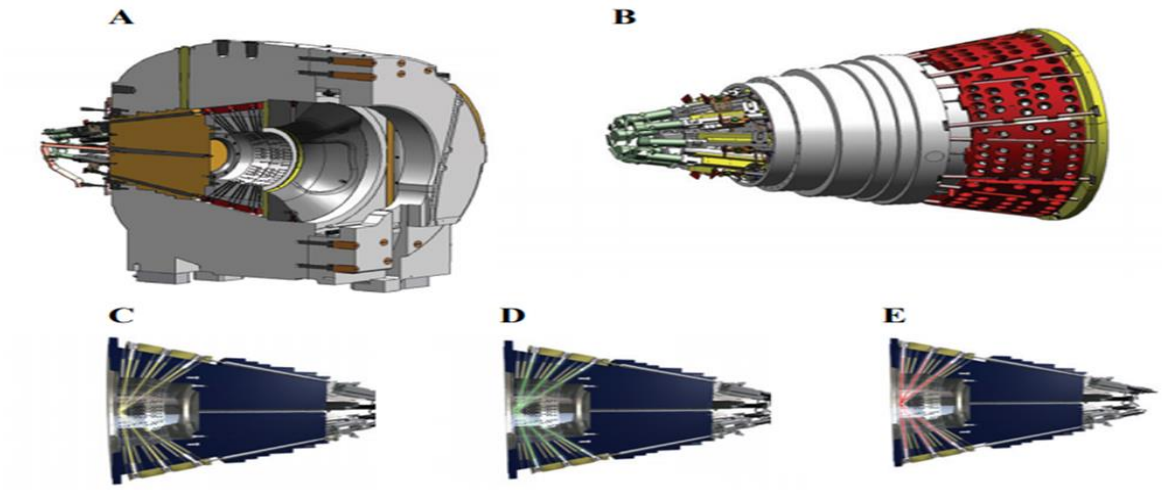

Figure (8): Gamma Knife Perfexion radiation unit and collimator system by Leksell. A) The Leksell Gamma Knife Perfexion radiation unit in cross section. B) A detailed view of the sectors; each sector has 24 60Co sources and can be moved independently of the other sectors to determine a collimator size or block beams. C) A sector location that defines a 4 mm collimator. D) A sector location that defines a collimator of 8 mm. E) A sector position that defines a collimator of 16 mm. (Elekta Instrument AB, Stockholm, Sweden, granted permission for the photos.)

A sector can also be placed between two rows of collimators, allowing individual sectors to be blocked during treatment. Using a skull immobilization device and a completely automated patient positioning system, the collimated beams are converged with great accuracy to a fixed isocenter where the target is positioned during treatment. [9]

4. The Advantages of Gamma Knife

Gamma knife Radiosurgery has various advantages over conventional surgery, some of them are mentioned below:

1-There is no need for any type of surgical incision on the patient's body, thus there is no postoperative pain, no blood loss, and no surgical site infection.

2- It is an outpatient treatment that takes about a day to complete.

3- Patients can continue their usual activities the next day.

4- It is less expensive than traditional surgery.

5- It reduces the length of post-surgical hospital stays.

6- Gamma knife surgery has been shown to be efficient in a number of deep-seated malignancies that are difficult to treat with traditional surgery.

7- It has a high degree of precision. [10]

5. Physics of Gamma Knife

The Leksell Gamma Knife versions (Icon, Perfexion) administer dosage from 192 Cobalt-60 sources collimated into narrow beams by a massive tungsten body. About 40 cm from the sources, the beams

converge in a narrow space known as the isocenter. The sources are divided into eight sectors, each with 24 sources. The sectors may slide in four different locations across the collimator body, which has 576 collimator channels in total, to produce beams with sizes of 4, 8, and 16 mm (The sizes refer to the cross-sectional diameters of single beams at the isocenter).When only a little amount of radiation seeps through the tungsten body, the fourth position is beam-off. There are 65,535 different beam size combinations for each isocenter, often known as "shots." A dose is administered to numerous isocenters by adjusting the patient's posture. As a result, the total dose can be molded to conform to the goal with a sharp dose gradient outside the target, resulting in a small dose for healthy tissue and organs at risk [11].

Due to the intersection of the 192 beams in an isocenter and the relatively sharp dose fall-off for single beams, a very high dose is delivered at the target, while the surrounding tissues are relatively spared. The patient's couch can be moved in relation to the isocenter to reach any point in the brain; and the shape and size of the focal volume can be optimized thanks to a unique collimator, divided into 8 sectors. Each sector can be moved to different positions: `Home' is the position when the system is switched off, `4 mm', `8 mm' and `16 mm' correspond to the 3 possible treatment configurations, and `Off' is an intermediary shielding position when the system is on but the patient's couch is being moved[12].

5.1 The impact of cobalt-60 source age on biologically effective dose in high-dose functional Gamma Knife radiosurgery

The influence of radiation dose rate on biologically effective doses (BED) has long been known, yet this effect is often overlooked when GKRS treatments are planned. The time it took for the target tissue to perform intrafraction DNA repair had a significant impact on the size of the BED change anticipated by the model. If intrafraction DNA repair is low (i.e., DNA repair halftimes are significantly longer than the irradiation period), the BED should be unaffected by cobalt-60 source age.

In most cases, GKRS is employed in practice for tumor care, with radiation doses of less than 30 Gy being used in most cases. Because the irradiation period in GKRS for tumors is often less than the time necessary for significant DNA repair in the target tissue, variation in cobalt-60 source age may be less important in tumor management given these lower doses and shorter treatment times. Functional GKRS treatments, on the other hand, can take hours, and the length of irradiation time varies dramatically depending on the age of the radiation source. The literature on DNA repair timeframes shows that cobalt-60 source age variation may be clinically important for high-dose functional GKRS.

The stronger the correlation between source age and BED, according to the model's results, the higher the prescription dose (and the longer the treatment time).For the same physical dose prescription, using a new cobalt-60 source after replacing an old source significantly increases the estimated (BED) for functional GKRS treatments. In the investigation of outcomes after high-dose functional GKRS treatments, source age, dosage rate, and treatment period should all be taken into account. To investigate how this potential shift in BED contributes to GKRS toxicity and whether technical adjustments should be made to reduce dose rates or prescription doses with newer cobalt-60 sources, animal and clinical investigations are needed [12].

5.2 Radiation around the Leksell Gamma Knife

Spectroscopic measurements revealed that during treatment, photons with energies less than 1150 Kev make up 81% of the dose in the area in front of the Gamma Knife. Primary photons account for less than 20% of the dosage, and the National Council on Radiation Protection and Measurements (NCRP)

assumption that the dose load is entirely made up of primary photons appears to be inaccurate. During treatment, the largest dose rate is logically present in front of the Gamma Knife, at an angle of around 30 degrees. When the system is turned off, however, the largest leakage appears to lie behind the Gamma Knife. The patient is within the unit during treatment, and all beams intersect in the brain target volume. The patient's scattered radiation makes up the majority of the radiation field in the room. The workload is 600 Gy/week (15 patients, each receiving a maximum dose of 40 Gy), and the occupancy factor is 0.075, equal to three hours of therapy per week. More than 50 cm of concrete is necessary to hide 40 hours of leakage per week, according to the NCRP method. There is no venture in saying that the NCRP method probably overestimates the leakage level around the Gamma Knife. The NCRP assumes that the radiation comes from a single source, is isotropic, and only consists of primary photons with energies of 1.25 MeV (mean energy of the two Co-60 gamma-rays), with leakage radiation accounting for 0.1% of the useable beam. In actuality, the Gamma Knife is surrounded by enormous casing and doors that screen the majority of the radiation from the 60Co sources, and leakage is significantly lower than the estimated 0.1%.

The Gamma Knife's design also prevents any primary photons from leaving the device without passing through the internal shielding, lowering the number of primary photons in the treatment room. Furthermore, the NCRP provides no guidance on how to aggregate the contributions of the 192 sources, and the radiation field produced by these almost 200 sources confined within a massive shielding case is highly anisotropic. As a result, the NCRP recommendations appear inadequate for the Gamma Knife system, prompting the creation of a new approach to structural shielding design [12].

5.3 Radioactive source Co-60

Cobalt was discovered by Georg Brandt, a Swedish chemist, in 1735. Cobalt-60 is artificially produced by bombarding a target material, either cobalt-59 or nickel-60, with neutrons. This reaction is produced by nuclear reactors. Natural Cobalt, Cobalt-59, has 27 protons and 32 neutrons. When inserted in a stream of slow neutrons, Cobalt- 59 absorbs a neutron and becomes Cobalt-60, which is radioactive. It emits an electron, a β-particles, from the nucleus and is transformed from Cobalt-60 to Nickel-60 [13]

The radiation source in the Leksell Gamma Knife treatment machine is cobalt-60, a radioactive isotope. When Co-60 decays, it produces beta particles as well as two strong gamma rays, one with 1.17 MeV of energy and the other with 1.33 MeV of energy.1 electron volt is the energy obtained by an electron that accelerates through a potential difference of 1 V. MeV is a widely used unit of energy for particles in the treatment energy range. The Gamma Knife's effective energy is slightly less than 1.25 MeV (the average of 1.17 and 1.33 MeV).Cobalt-60 decays to nonradioactive nickel in the end. The half-life of Co-60 is 5.26 years, which is the amount of time it takes for Co-60 to lose half of its radioactivity due to decay. Only half of the original radioactive material remains at the end of one half-life. This means that after 5 years, treatment time is double what it was when the system was first installed, and that the Gamma Knife source must be replaced after a certain amount of time to prevent long treatment times gamma knife capsule is show in fig(9).

The decay scheme of a cobalt-60 nucleus that has been made radioactive in a reactor by bombarding stable Co-59 atoms with neutrons is shown in the diagram below in figure (10). [12]

Figure (9): gamma knife capsule (neuroscience hospital, GK center, Baghdad, Iraq).

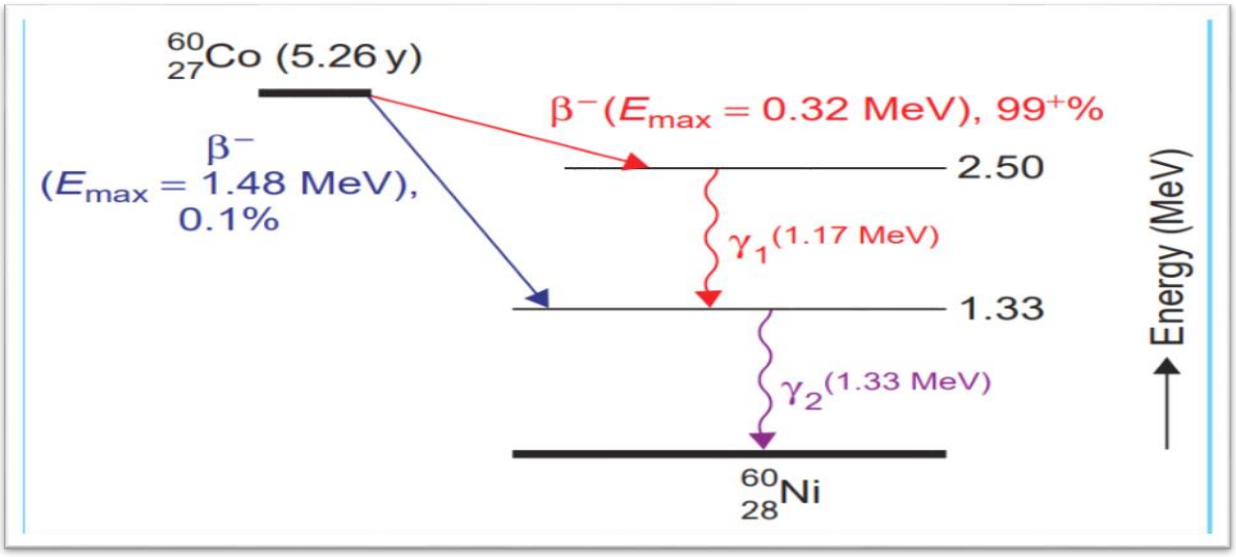

Figure (10): cobalt-60 scheme decay

6. Patient's preparation procedure

To assure that the treatment is done properly, the following measures were taken to the patient for the treatment

6.1 Stereotactic frame fixation

The fixation frame is attached to the patient's skull under local anesthesia on the day of the treatment. The frame has two crucial functions: First off, it has a rigid fixing technique that prevents the patient from moving throughout the delivery. Second, it provides a frame of reference for determining tumor localization relative to the frame and the delivery unit.

Starting to put a stereotactic frame. The frame is fixed to the patient's head with four screws after a little sedation is taken. This process, which is done under local anesthetic, takes around five minutes. Figure (11) illustrates the frame. [14]

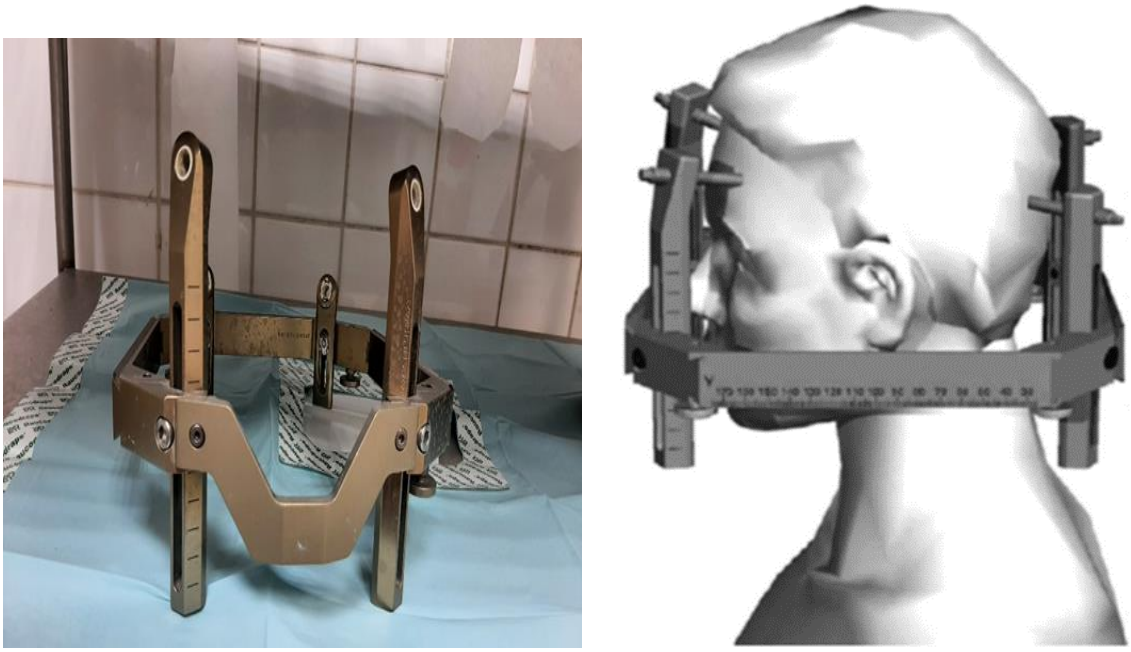

Figure (11): Gamma knife coordinate frame

6.2 Anesthesia

Before fixing the frame over the head with a screw we should use Local anesthesia, where this anesthesia is injected through the plastic inserts for each frame attachment. The anesthetic which was used in this process is called lidocaine, fig (12) show the needle of lidocaine and fig (13) show the patient taken the local anesthesia.

The surgeon should be informed of previous craniotomies, burr holes, and shunts so that no local anesthetic or pins are used there. [1]

Figure (12): Picture of the needle of the local anesthetic.

Figure (13): picture of the patient when taken the local anesthesia

6.3 Fixation of frame screw

Fixation Screws are utilized to fix the Leksell Coordinate G Frame to the patient's skull. Aluminum is used to make these fixing screws, the medical-grade titanium allows for a long lifetime. Long-lasting and durable hexagonal fixation screws allow for enhanced treatment volume in the Leksell Gamma Knife and simplicity of usage in confined MR head coils. During MRI scanning, always employ Insulated Fixation Posts. The screw has a hexagonal socket. This allows for flush mounting with the frame posts while also providing optimal frame stability. The Fixation Screws package includes 20 pairs of reusable screws in various lengths.as shown in fig (14).

Figure (14): Sterilizing case with slots for all Elekta fixation screw lengths available, and fixation screw

To fix the frame to the patient's head, use a socket wrench in conjunction with Fixation Screws (see figure 15). For the frame to be safely secured, two Socket wrenches are required. [3]

Figure (15): picture of socket wrench (neuroscience hospital, GK center, Baghdad, Iraq)

6.4 Fitting the Frame cap

The Perfexion further utilizes a "frame cap" (Figure 16), which conservatively simulates a human scalp and is of known dimensions to the treatment planning system.

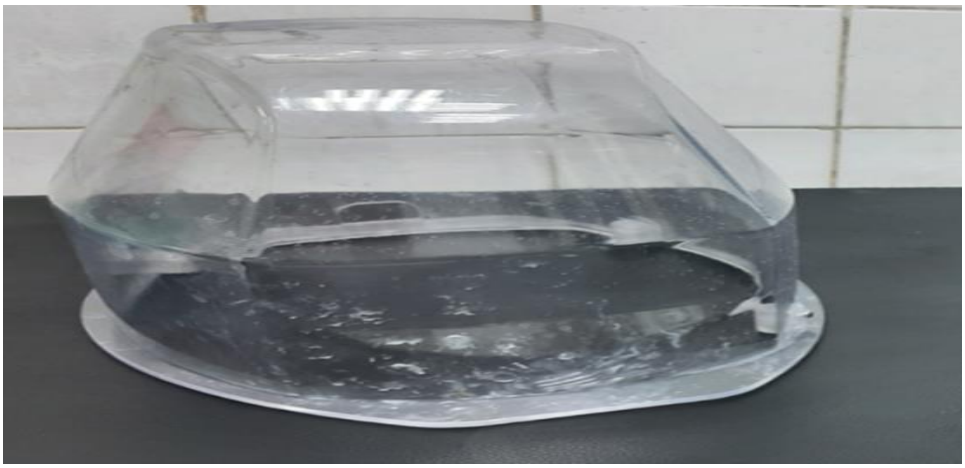

Figure (16): The Frame cap

The frame cap is placed over the stereotactic frame and allows the system to reduce the chance of collisions in many cases, lowering the number of skull and frame measurements requested. Finally, the Perfexion includes a collision sensor in the shape of an aluminum cap that covers the treatment cavity. When pressure is applied to this cap, the system will retract the sources to their protected home position, reducing radiation exposure and allowing the patient to be manually removed from the unit. [2]

6.5 Fitting the indicator

CT imaging is a less widely used imaging technique due to its poor soft-tissue visibility. CT imaging, on the other hand, is highly effective in circumstances where MR is contraindicated or where the bone structure may provide important information. During CT scanning, the Open CT Indicator is utilized in conjunction with Leksell Coordinate Frame G for target localization in stereotactic neurosurgery, radiosurgery, or stereotactic radiotherapy. It has an open top that allows for a lower frame mount as in fig (17). [3]

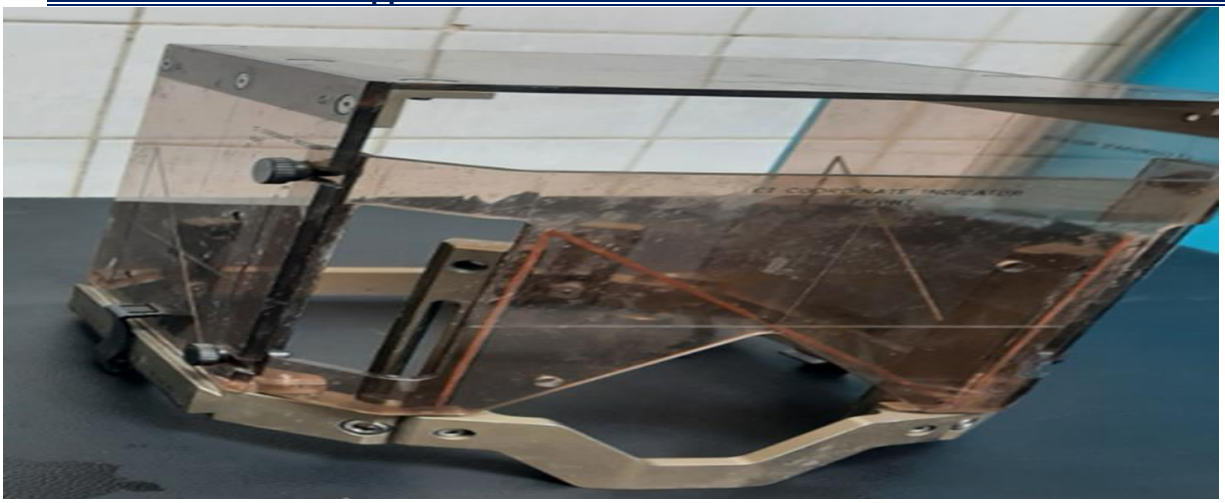

Figure (17): CT indicator

MR Indicator with five side plates is used in stereotactic neurosurgery and radiosurgery during MR scanning for target localization. [3]

The MRI fiducially system is made up of a plastic box that is directly attached to the stereotactic frame (Figure 18). Channels with a characteristic "N" shape are machined into the box. A cupric sulfate solution injected into the channels to improve commonly utilized pulse sequences. The fiducially marks emerge as a series of dots in the image when resampled as axial and coronal sections.

Figure (18): MRI indicator

It should be indicated that MRI is sensitive to a wide range of linear and nonlinear geometric distortions, mainly caused by gradient field nonlinearity and magnetic field in homogeneities, including those caused by the patient and frame. [2]

6.6 Radiographic imaging

Following the installation of the head frame, the patient will be subjected to an MRI or CT scan, depending on the diagnosis. These radiology scans are taken to precisely detect the size, form, and location of your tumor, lesion, or irregularity. The head frame will be fitted with an indication box. When the imaging studies are finished, the patient can take a seat while the neurosurgeon, radiation oncologist, and physicist use the images to arrange the treatment. [15]

6.7 Skull-scaling measurements

In order to compute photon attenuation and avoid collisions between the patient and the unit, the Gamma Knife treatment planning system requires the depth of the target point in each beam direction.

Gamma Plan does this by collecting sampled skull measurement data with skull scaling equipment Figure (19), which is then interpolated and used to generate the appropriate skull and frame model. A member of the treatment team measures the distance from the scaling "bubble" to the patient's head with a simple ruler and enters this information into the treatment planning system. [2]

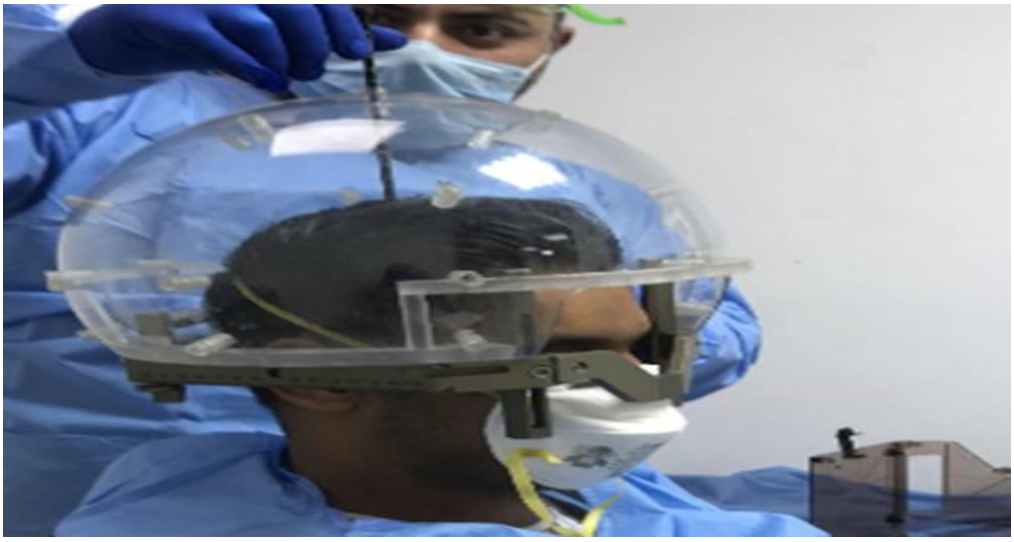

Figure (19): picture of A physicist takes a measurement of the patient's skull.

6.8 Image registration

In this study, we used two approaches: patients who had previously undergone GK SRS (under follow up) used the first approach (figure 20), while patients who underwent all treatment procedures with us used the second approach, in which stereotactic CT scanning was performed using a fiducially system when acquiring the images. The MRI images are then registered to the CT dataset and mapped into stereotactic space. There is no significant effect from employing any of the approaches, but the crucial thing is to do imaging for the patient while wearing the frame to identify patient skull coordinates. The fiducially differences between CT and MRI are shown in (Figure 21). [4]

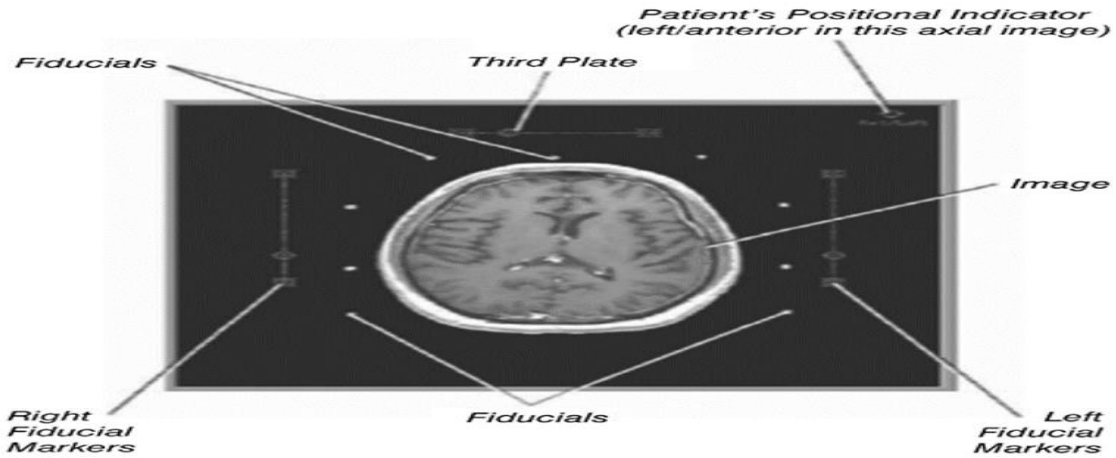

Figure (20): MRI image of a Gamma Knife patient, fiducially marks appear as white spots (Photo courtesy of Elekta).

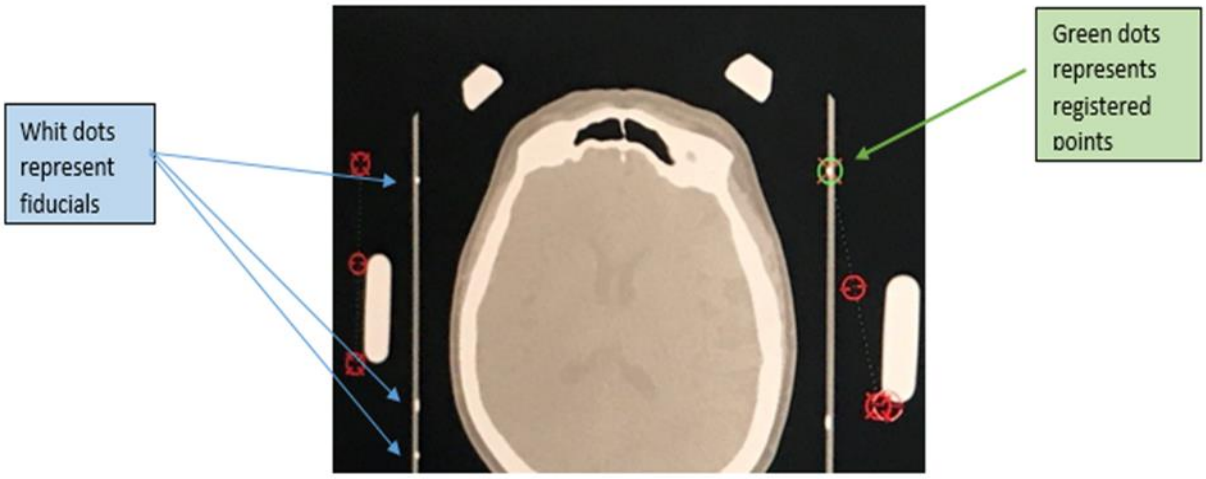

Figure (21): The fiducially markings on the CT scan appear smaller than those on the MRI picture (neuroscience hospital, GK center, Baghdad, Iraq).

6.9 Prescribed treatment dose

This entailed entering the prescribed dose (12-20) Gy into GK's planning software in single or several shots. The neurosurgeon performed this step, as well as all subsequent processes until the data was exported to the LGK treatment interface. The dose of 12 Gy is regarded a minimum dose to create any control for tumor size as advised by the GK Society, and it is used in Neuroscience Hospital Center, Baghdad, Iraq.

6.10 The prescription dose ranges

The prescription dose ranges (minimal dose to target volume) for critical structures for single fraction Leksell Gamma Knife treatment shown in (Table 1).

Table (1): Special limits for maximal point doses and mean doses to critical structures for single fraction Leksell Gamma Knife treatment

Critical structure	Maximal point dose Gy
Optic nerve	8-10
Brainstem	12-15
Eye lens	2

Cornea	10
Eyelid, conjunctiva	10
Infundibulum	17
Pituitary gland	15 (Maximal mean dose)
Cochlea	4.5 (Maximal mean dose)

6.11 Determination of target's isocenter

Target decides to create a conformal plan. The LGP (Leksell Gamma Planning) program (manual or semiautomatic mode) can be used to outline the target volume (see figure 22). The target determination technique is used for more precision, delineation, and outlining of the target.

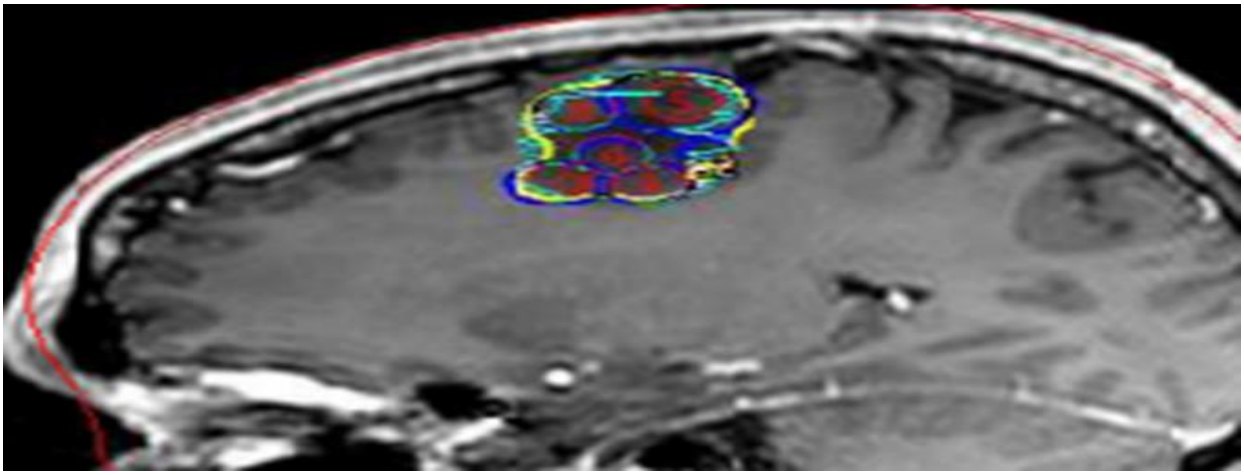

Figure (22): Target determination of low grade glioma with multiple shots (neuroscience hospital, GK center, Baghdad, Iraq)

6.12 Dose targeting

This phase was taken to improve patient treatment safety by using sector channels "plugging" of the GK device to prevent dose from vital components such as the optic nerve, optic chiasm, and brainstem while giving dose to cover the larger extent of the adenoma. Figure (23) shows how the weight of the shot was reduced or raised to provide better protection to the essential organs, figure (24) shown the screens with all setting steps. [4]

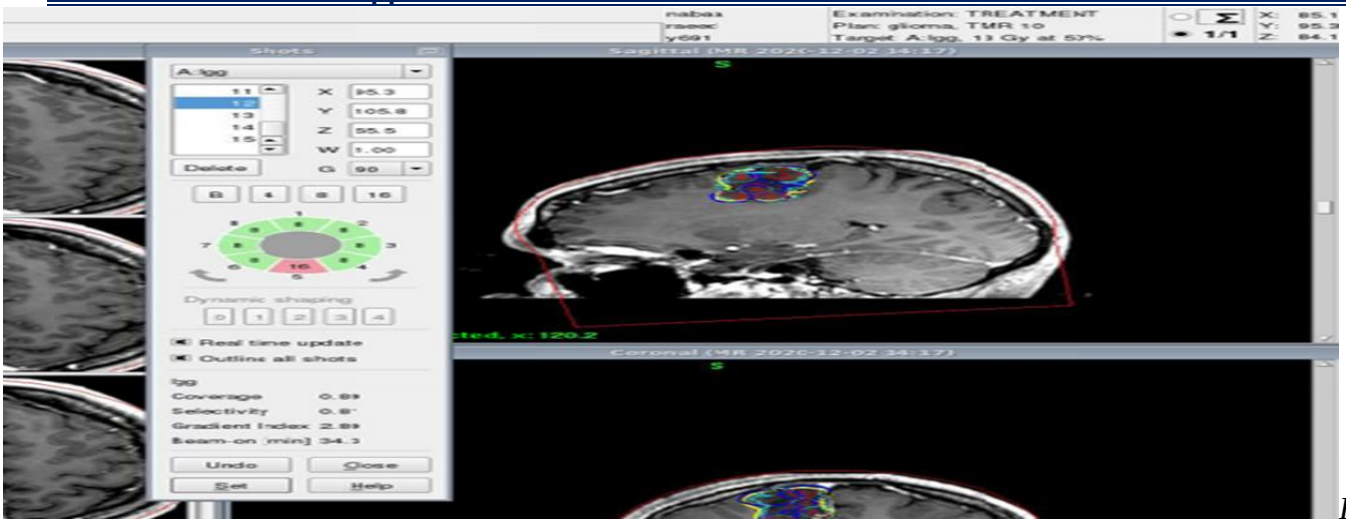

Figure (23): The usage of plugging blocks and GK weight to decrease dosage to healthy tissue (neuroscience hospital, GK center, Baghdad, Iraq).

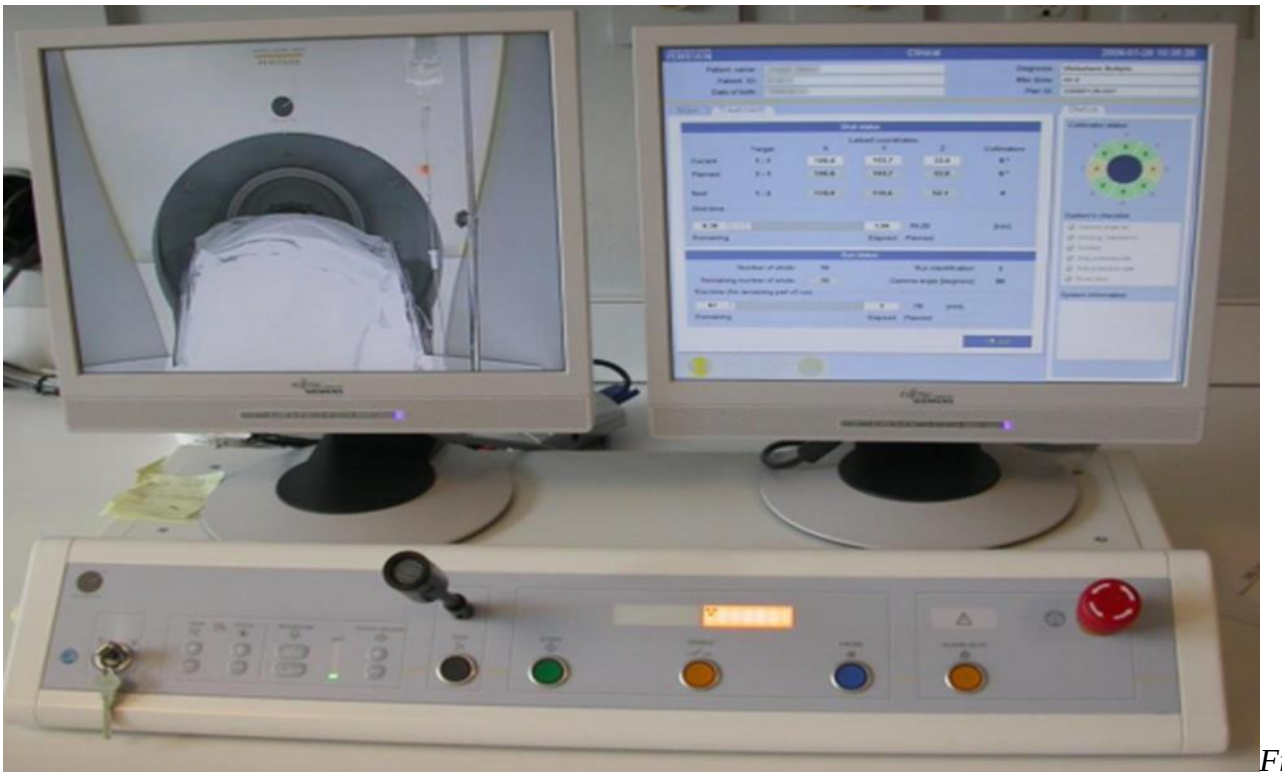

Figure (24): shown the screens with all setting steps, it can be found installed inside the device unit.

6.13 Patient Irradiation

Finally, after plan approval, protocol printing, and data export to the LGK treatment console. The patient was then placed on the couch to undergo radiation treatment after the whole patient data was imported into the LGK treatment control system.

To begin this final step, there are several settings to the patient on the couches before closing the door (as indicated in figure 25):

1. Gamma angle 900.

2. Docking standard G.

3. Docked.

4. Side protection left & side protection right.

5. Close the room door. [6]

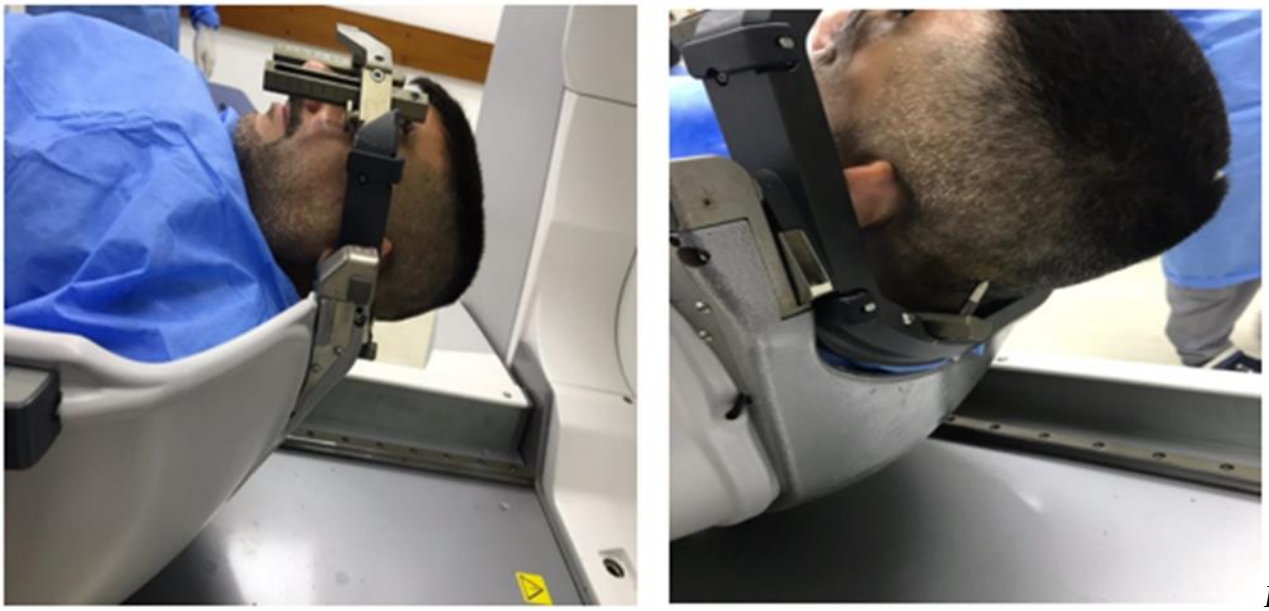

Figure (25): A patient on a couch in a medical setting (neuroscience hospital, GK center, Baghdad, Iraq)

7. Patients' Follow-Up:

Six months after treatment; the evaluation was based on knowledge of the effect of radiation on size. The follow-up includes MRIs for all patients who treated by GKRS, as well as measurements of tumor size before and after GK for all patients.

8. References

[1] J. Greenberg, L. Dade Lunsford, and A. Niranjan, “Anesthesia considerations during Leksell radiosurgery,” Prog. Neurol. Surg., vol. 34, pp. 63–72, 2019, doi: 10.1159/000493051.

[2] D. J. Schlesinger, C. P. Yen, C. Lindquist, and L. Steiner, “Gamma Knife: Technical Aspects,” Textb. Stereotact. Funct. Neurosurg., pp. 897–928, 2009, doi: 10.1007/978-3-540-69960-6_58.

[3] N. Product and S. Catalog, “Neuroscience Product & Services Catalog.”

[4] D. Schlesinger, “The Effectiveness of the Prescribed Dose of the Gamma Knife Radiosurgery in Treating Secretory Pituitary Adenomas,” Solid State Technol., vol. 63, no. 5, pp. 3579–3595, 2020.

[5] D. Schlesinger, “Historical and Technical Overview of Gamma Knife Radiosurgery Disclosures Research support : Elekta , AB.”

[6] R. D. A. Al Qader, R. S. Ahmed, and Y. M. Hassan, “The Effectiveness of the Prescribed Dose of the Gamma Knife Radiosurgery in Treating Secretory Pituitary Adenomas,” Solid State Technol., vol. 63, no. 5, pp. 3579–3595, 2020.

[7] A. Bertalanffy et al., “Gamma knife radiosurgery of acoustic neurinomas,” Acta Neurochir. (Wien)., vol. 143, no. 7, pp. 689–695, 2001.

[8] I. Yang et al., “Facial nerve preservation after vestibular schwannoma Gamma Knife radiosurgery,” J. Neurooncol., vol. 93, no. 1, pp. 41–48, 2009.

[9] D. Kaul, V. Budach, L. Graaf, J. Gollrad, and H. Badakhshi, “Outcome of elderly patients with meningioma after image-guided stereotactic radiotherapy: a study of 100 cases,” Biomed Res. Int., vol. 2015, 2015.

[10] A. Ö. Börcek et al., “Gamma Knife radiosurgery for arteriovenous malformations in pediatric patients,” Child’s Nerv. Syst., vol. 30, no. 9, pp. 1485–1492, 2014.

[11] C. J. De Vile et al., “Management of childhood craniopharyngioma: can the morbidity of radical surgery be predicted?,” J. Neurosurg., vol. 85, no. 1, pp. 73–81, 1996.

[12] L. S. Chin and W. F. Regine, “Principles and practice of stereotactic radiosurgery,” Princ. Pract. Stereotact. Radiosurgery, pp. 1–842, 2015, doi: 10.1007/978-1-4614-8363-2.

[13] IAEA, “Identification of Radioactive Sources and Devices,” Iaea, no. September 2007, pp. 1–154, 2007.

[14] L. S. Chin and W. F. Regine, Principles and Practice of Stereotactic Radiosurgery. 2008.

[15] R. Liščák, “Gamma knife radiosurgery,” Gamma Knife Radiosurgery, pp. 1–326, 2013, doi: 10.1097/00007611-199005000-00016.

ISSN (Print): 2958-8987
ISSN (Online): 2958-8995
Doi: 10.59799/APPP6605

An Application on Principal Components Analysis using R

Qasim N.Husain[1], and Alaa M.Dedaa[2]

[1] Department of Mathematics, College of Education for Pure Sciences, Tikrit University, Tikrit ,IRAQ;
E-mail: qasim11@tu.edu.iq

[2] Department of Mathematics, College of Education for Pure Sciences, Tikrit University, Tikrit ,IRAQ;
E-mail: alaa.m.dedaa@st.tu.edu.iq

Abstract:

This study suggests using three exploratory data analysis steps (Data Summarization, Data Visualization, Data Normalization) on a functional data set. The data used in this research is Canadian weather data. Principal components analysis process for the data are used the command (prcomb) from the software R to reduce the analysis time and display more accurate results. New codes are established to analyze functional data, and then the data are represented using functional boxplot , histogram, and barplot techniques.

Keywords: Exploratory Data Analysis**,** Functional Data Analysis**,** Exploratory Functional data Analysis**,** Functional Boxplot**,** Principal Components Analysis.

1. Introduction

The researcher's ability to analyze raw data is very important skill due to the growing interest in data analysis in many areas of life such as environment, medicine, politics, psychology and many others disciplines. One of the most important methods of data analysis is exploratory data analysis and functional data analysis, which have recently begun to work together. in several statistical areas.

(Jolliffe, 1986) introduced the principal component analysis as an exploratory and functional tool used to reduce data dimensions while preserving as much variance as possible. It is a simple and very common method among multivariate statistical techniques, several applications have been used and applied in R statistical program and using of special codes to facilitate the solution and greatly save time and effort.

2. Basic Concepts

Definition 2.1 Functional data analysis (FDA) is a term coined by Ramsay in (1982), but its history dates back to Grenander in (1950). It is a statistical method for analyzing data and representing it in curves or surfaces. the technique is a intrinsically infinite dimensional ,and is a rich source of information in data analysis, looking at observations as functions and each sample considers it a random function. It has a great importance in the fields of medicine, environment, meteorology and economics.

Definition 2.2 Exploratory data analysis (EDA) is a statistical technique for data analysis introduced by Tukey in (1977). The term EDA is defined to depict the data analysis philosophy by introducing set of graphical and numerical summaries as well the structure of the data are explained. The relationship between the variable and the data trends are specified and represented graphically.

Definition 2.3 Principal components analysis (PCA) can be defined as a technique for reducing variables and it is used to analyze, simplify, and processing data. . PCA technique is considered as a standard instrument applied on multivariate data analysis to minify the dimensions during preserving the data variation. PCA Measures how each variable is associated with one another by using a Covariance matrix . It is used in many applications as stock market predictions data, and many others . PCA in its essence can be considered an exploratory tool in addition to being a widespread tool in the field of functional data.

Definition 2.4 Functional boxplot (FBP) is an exploratory tool for analyzing, generalizing and visualizing functional data. It is created similar to a regular boxplot .

Definition 2.5 Outliers: is an observation that lies an abnormal distance from other values in a random sample.

3. Methodology

To perform an EFDA in R, we take a functional data set and perform an exploratory analysis on it, There are three stages of EDA. The first stage is data summarization, the second stage is data visualization, and the third is data normalization. Before starting the analysis steps in R, the data packages for EDA are downloaded, which is the statistics package (“stats”) that contains functions for data exploration and a deep lie package ("dplyr") which contains functions for data manipulation, and packages for FDA, which is ("fda") which contains the data set to be worked on with commands for FDA and package ("fields"). After installing the statistical packages, and loading the data, An exploratory analysis is started, where the data is summarized by creating a group that contains the data and selecting the variable to be analyzed from it, then calculating the different measures of the data (mean, median, mode, standard deviation and variance, as well as the quartiles).

After summarizing the data, the second stage of the exploratory analysis begins, which is data visualization. It depends on the type of data where histogram of numerical data and boxplot for categorical data. The data structure is shown to see the types of data, and then choose the method of representation for each type of data. the last stage, which is data normalization, where the variables are normalized for the data set by calculating the (z-score) scale, It uses numerical data only, and displays the results (z-score) , this is the last step of the exploratory data, then principal components analysis of the data , which is a functional exploratory method of data analysis.

4. Example: Canadian Average Annual Weather Cycle

In this example, an EDA for FDA using Canadian weather data by PCA are applied

First the data set and some packages of EDA and FDA have been loaded

So, downloading fda and calling the data names (ME) as follows:

```
> ME<-Canadian Weather
#1- data summarization
command str to show structure of data
> str (ME)
take the monthly temp as
>sl=ME$ monthly Temp
The mean of data
>mean(sl)
[1] 1.801284
>median(sl)
[1] 3.963333
To load mode use first
mode=function(x){
  ta=table(x)
  tam=max(ta)
  if(all(ta==tam))
    mod=NA
  else
    if(is.numeric(x))
      mod=as.numeric(names(ta)[ta==tam])
  else
    mod=names(ta)[ta==tam]
  return(mod)
}
Then we find mode
>mode(sl)
[1] -8.16129 10.66000 11.62333 20.82903
```

To find standard derivation of AM

> sd (sl)

[1] 12.69994

>var (sl)

>quantile(sl)

0%	25%	50%	75%	100%
-33.007143	-6.630645	3.963333	12.410484	20.829032

>dim(sl)

[1] 12 35

To show the boxplot of sl

>boxplot(ME $ monthly Temp)

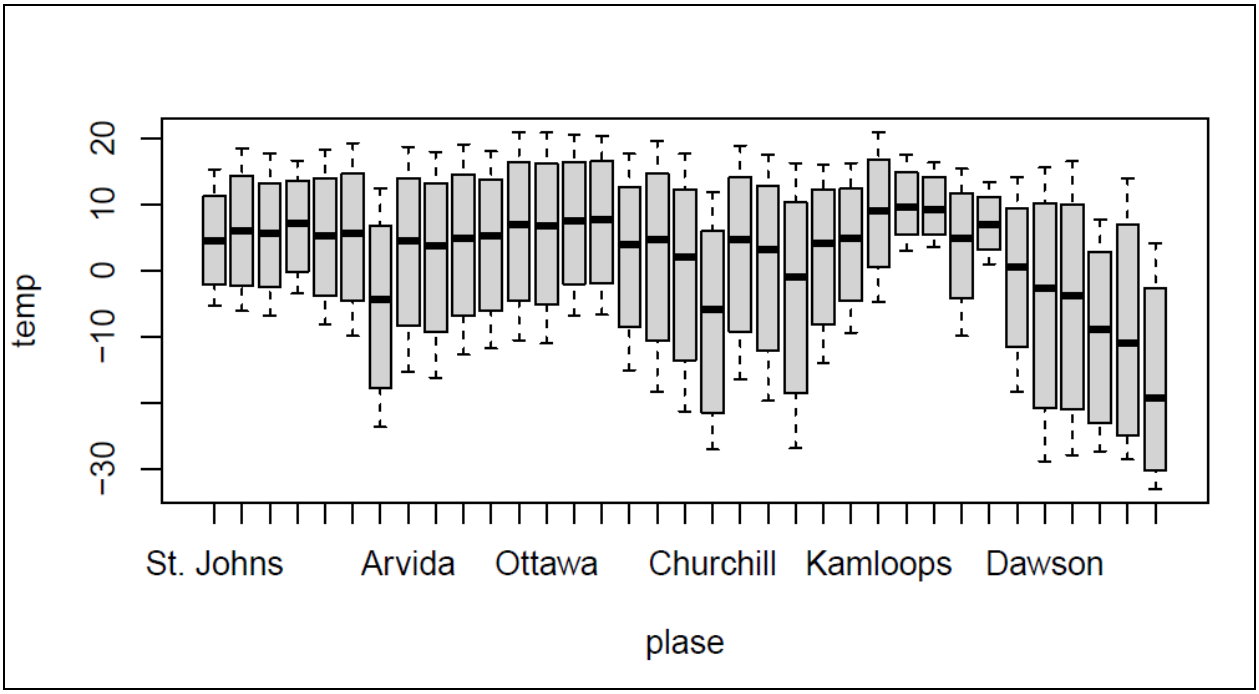

Figure 1: Box plot of monthly temperature

#2- data visualization (histogram for numerical data)

>hist(sl)

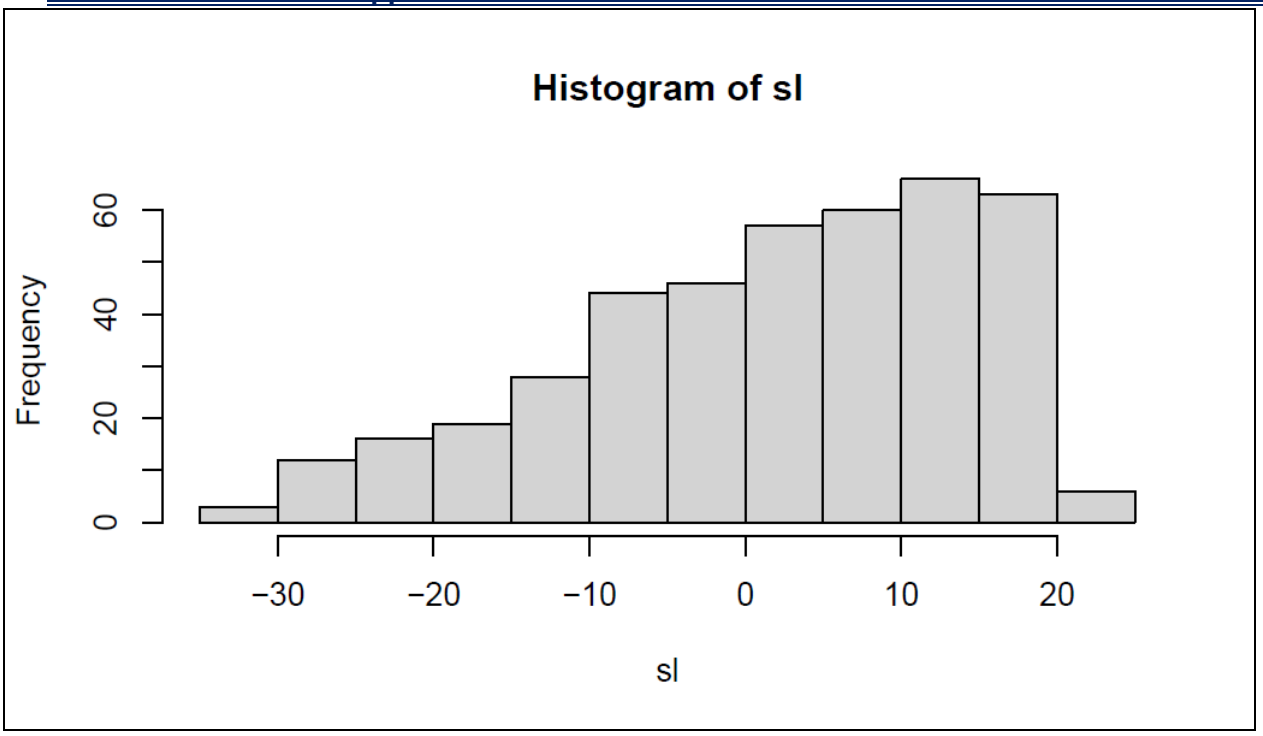

Figure 2: Histogram of data

#(barplot for categorical data)

> da<-md $region

>table(da)

Arctic	Atlantic	Continental	Pacific
3	15	12	5

>bar plot (table(da))

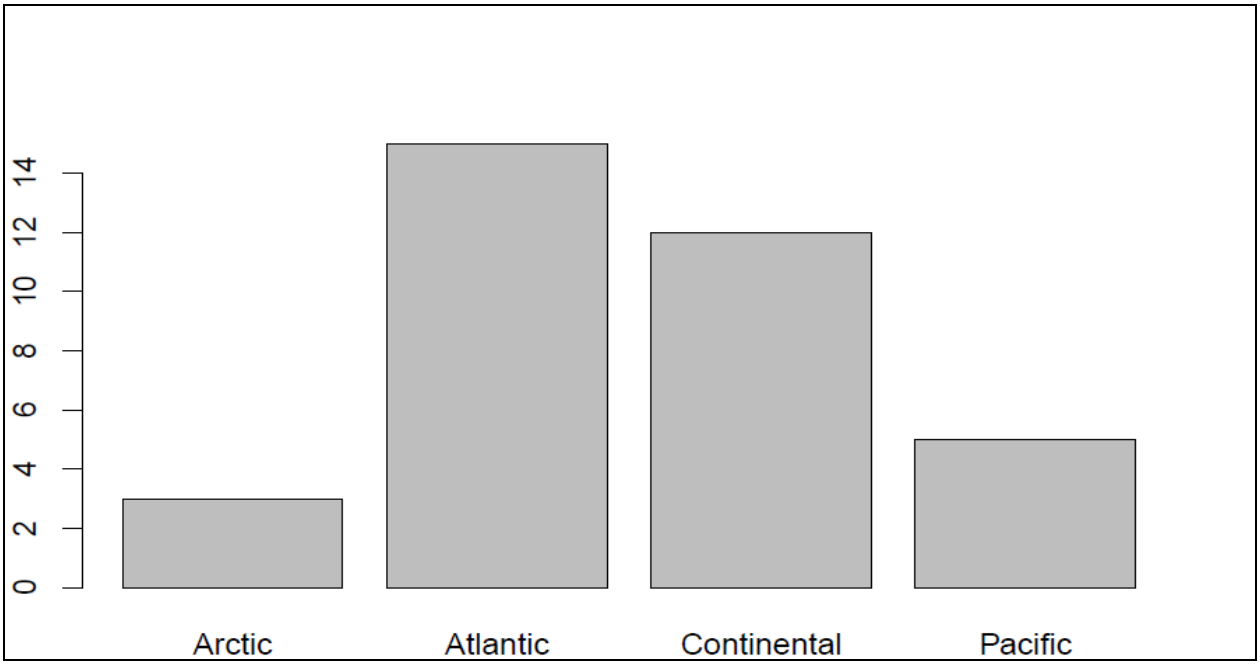

Figure 3 bar plot of region(categorical data)

#3- data normalization

md_numeric<-(md$dailyAv)

zscore_md<-scale(md_numeric)

#PCA for EFDA

> pc=prcomp (sl,scale=TRUE)

>summary(pc)

Table 1 summary of PC data

Importance of components:						
	PC1	PC2	PC3	PC4	PC5	PC6
S.D	5.8659	0.63270	0.36144	0.19532	0.11548	0.05866
Var.	0.9831	0.01144	0.00373	0.00109	0.00038	0.00010
Cnm.	0.9831	0.99455	0.99828	0.99937	0.99976	0.99985
	PC7	PC8	PC9	PC10	PC11	PC12
S.D	0.04670	0.03986	0.02538	0.02252	0.01428	2.308e-16
Var.	0.00006	0.00005	0.00002	0.00001	0.00001	0.000e+00
Cnm.	0.99992	0.99996	0.99998	0.99999	1.00000	1.000e+00

>plot(pc,type="l")

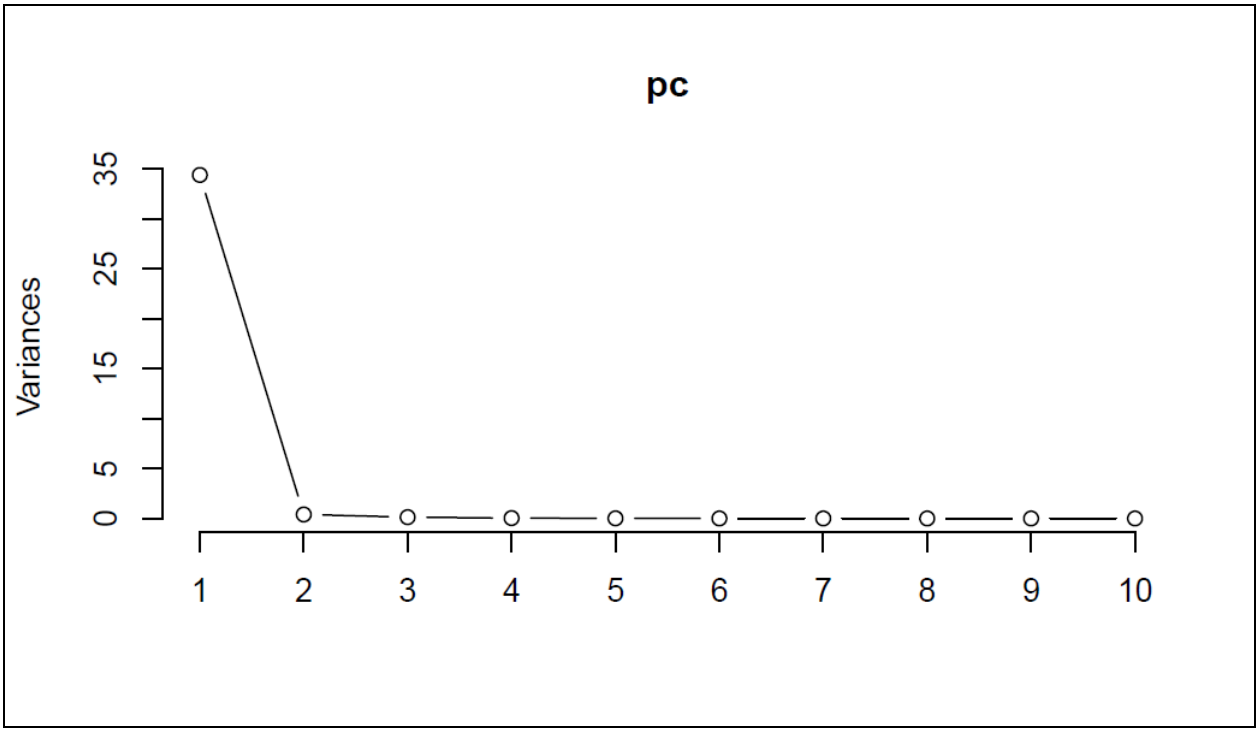

Figure 4 PCs as Line

>biplot(pc)

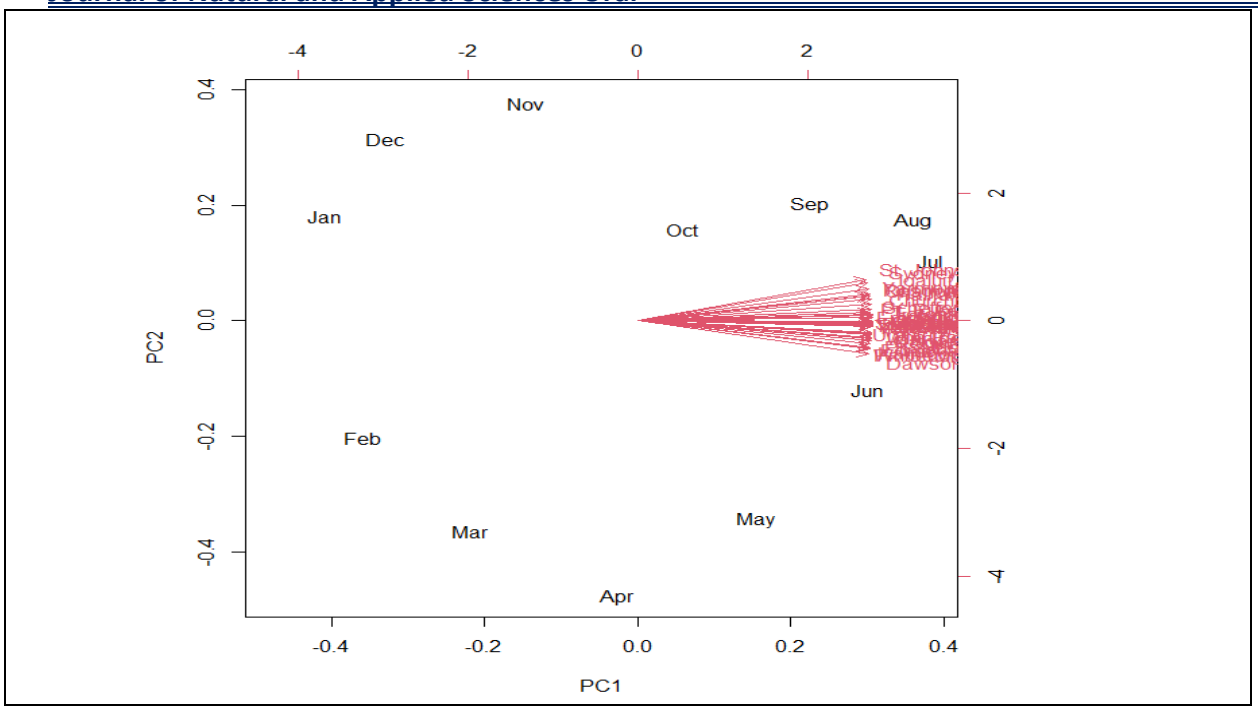

Figure 5 biplot of pc

>attributes(pc)

$names

[1] "sdev" "rotation" "center" "scale" "x"

$class

[1] "prcomp

>cor <-t(sl)

>pc$sdev

>pc$scale

> boxplot(pc$scale)

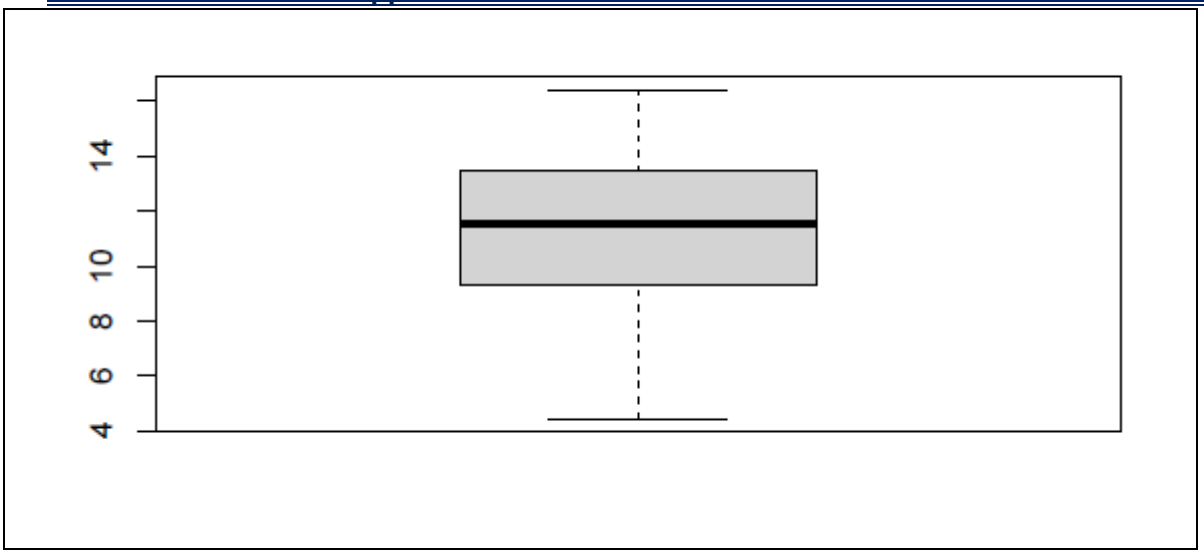

Figure 5: Boxplot of the scale of pc

> fbplot(sl,method='MBD',ylim=c(-2,20))

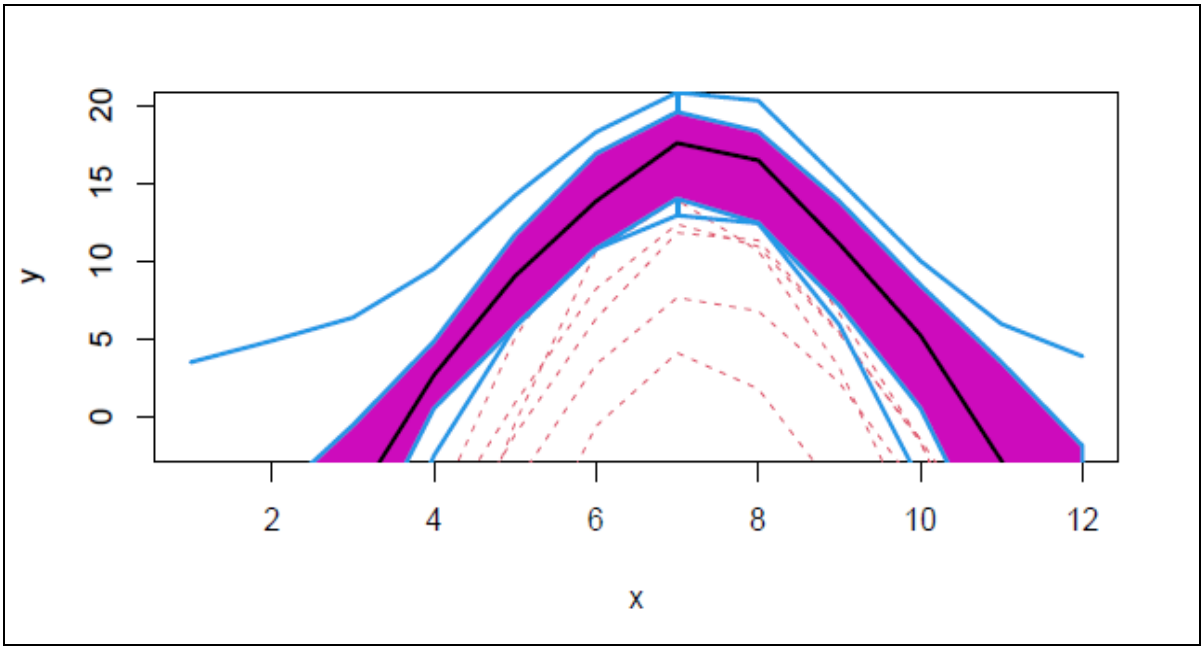

Figure 6: Functional boxplot of the data

4. Conclusion

In this research, the three steps of Exploratory Data Analysis were used in R program on Functional Data, which is Canadian weather data, and only numerical data was taken from it. The data was visualized using histogram to the numerical data and the barplot for the categorical data. The Functional boxplot was used.

Data normalization was done using z-scale. A principal component analysis of the data was done using the prcomp command, and the results were written in the form of tables and graphics.

References

- Adnan, N. I. M., Adam, M. B., Ishak, M. Y., Ibrahim, N. A., & Azmai, M. N. A. (2016). Functional Data Analysis for Extreme Data. Indian Journal of Science and Technology, 9, 28.
- Braun, W. J., & Murdoch, D. J. (2021). A first course in statistical programming with R. Cambridge University Press.
- Chebana, F., Dabo-Niang, S., & Ouarda, T. B. (2012). Exploratory functional flood frequency analysis and outlier detection. Water Resources Research, 48(4).
- Groth, D., Hartmann, S., Klie, S., & Selbig, J. (2013). Principal components analysis. In Computational Toxicology (pp. 527-547). Humana Press, Totowa, NJ.
- Holland, S. M. (2008). Principal components analysis (PCA). Department of Geology, University of Georgia, Athens, GA, 30602-2501.
- Horváth, L., & Kokoszka, P. (2012). Inference for functional data with applications (Vol. 200). Springer Science & Business Media.
- Jolliffe, I. (2022). A 50-year personal journey through time with principal component analysis. Journal of Multivariate Analysis, 188, 104820.
- Kassambara, A. (2017). Practical guide to principal component methods in R: PCA, M (CA), FAMD, MFA, HCPC, factoextra (Vol. 2). Sthda.
- Liu, Q. (2014). The application of exploratory data analysis in auditing (Doctoral dissertation, Rutgers University-Graduate School-Newark).
- Ngo, D., Sun, Y., Genton, M. G., Wu, J., Srinivasan, R., Cramer, S. C., & Ombao, H. (2015). An exploratory data analysis of electroencephalograms using the functional boxplots approach. Frontiers in neuroscience, 9, 282.
- Suarez, A. J. (2016). Bayesian Methods for Exploratory Functional Data Analysis and Existence Theorems for Solutions to Nonlinear Differential and Difference Equations.
- Tipping, M. E., & Bishop, C. M. (1999). Probabilistic principal component analysis. Journal of the Royal Statistical Society: Series B (Statistical Methodology), 61(3), 611-622
- Tukey, J. W. (1977). Exploratory data analysis (Vol. 2, pp. 131-160).